ANL/FE-85-14

THE ANL DOPPLER FLOWMETER

by

H. B. Karplus, A. C. Raptis,
S. Lee, and T. Simpson

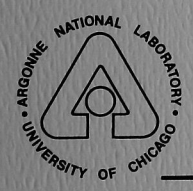

FOSSIL ENERGY PROGRAM

ARGONNE NATIONAL LABORATORY, ARGONNE, ILLINOIS

Operated by THE UNIVERSITY OF CHICAGO
for the U. S. DEPARTMENT OF ENERGY
31-109-Eng-38

Argonne National Laboratory, with facilities in the states of Illinois and Idaho, is owned by the United States government, and operated by The University of Chicago under the provisions of a contract with the Department of Energy.

Printed in the United States of America
Available from
National Technical Information Service
U. S. Department of Commerce
5285 Port Royal Road
Springfield, VA 22161

NTIS price codes
Printed copy: A05
Microfiche copy: A01

Distribution Category:
Coal Conversion and Utilization--
Coal Science and Analysis (UC-90a)

ANL/FE-85-14

ARGONNE NATIONAL LABORATORY
9700 South Cass Avenue
Argonne, Illinois 60439

THE ANL DOPPLER FLOWMETER

by

H. B. Karplus, A. C. Raptis,
S. Lee,* and T. Simpson**

Components Technology Division

October 1985

Prepared for U. S. Department of Energy
Office of Fossil Energy
Pittsburgh Energy Technology Center

*Pittsburgh Energy Technology Center, U.S. Department of Energy
**U.S. Department of Energy, Washington, DC

CONTENTS

CONTENTS (contd.)

LIST OF FIGURES

LIST OF FIGURES (Contd.)

LIST OF FIGURES (contd.)

LIST OF TABLES

GLOSSARY AND NOMENCLATURE

Compression acoustic wave — Propagation of a compression stress wave in a substance.

Cutoff frequency — For a band-limited noise spectrum (as obtained for the Doppler signal on laminar flow), the cutoff frequency is defined as the frequency at which the spectrum level is 3 dB (i.e., it has half the energy) below the peak level. For white noise the cutoff is twice the spectrum centroid.

Doppler shift — The difference of frequency between transmitted waves and the wave scattered by a moving particle.

Electronic mixer — A nonlinear device that generates a signal combining the properties of two inputs. It can be represented by a multiplication
$2\cos 2\pi f_t t \times \cos 2\pi f_r t = \cos 2\pi (f_t + f_r)t + \cos 2\pi (f_t - f_r)t.$

Mode conversion — Change from shear to compression waves (or the reverse) at an interface between two substances.

Octave — Two frequencies f_a, f_b are one octave apart when $f_a = 2f_b$ or $f_b = 2f_a$.

Rheological property of a fluid — The relation of the shear stress to velocity gradient in a fluid. (If the relation is linear the fluid is called a Newtonian fluid.)

Shear acoustic wave — Propagation of a shear stress in a solid. In an isotropic solid this wave propagates at right angles to the stress.

Slurry — A fluid containing solid particles in suspension.

Spectrum — The distribution in frequency of the magnitude of the component waves.

Tone — A simple harmonic acoustic wave (its spectrum is a single line).

White noise — A random disturbance with a uniform spectrum.

Zero crossing frequency — The number of times in one second in which a signal changes sign.

c	
c_f	
c_p	
c_w	
f	
f_t	
f_r	
f_d	
f_i	
f_o	
r_o	
$\dot{Q}$	
S	
u	
u_m	
$\bar{u}_s$	
$\bar{u}_{dia}$	
V	
V_o	
θ	

Velocity of acoustic (sound) wave

Velocity of acoustic (sound) wave in the fluid

Velocity of acoustic (sound) wave in the pipe wall

Velocity of acoustic (sound) wave in the coupling wedge

Frequency

Frequency of the transmitted wave

Frequency of the received wave

Frequency of the Doppler shift $f_d = |f_t - f_r|$

Cutoff frequency of band limited spectrum

Pulse repetition output of Doppler meter

Radius of the pipe

Volume flowrate of fluid

Sectional area of pipe

Flow velocity

Maximum u (on centerline of pipe for symmetrical flow)

Area averaged flow velocity $\dot{Q}/S$

Average value of flow velocity averaged along a pipe diameter

Voltage

Voltage output from flowmeter

Angle of sound beam with pipe axis

THE ANL DOPPLER FLOWMETER

by

H. B. Karplus, A. C. Raptis,
S. Lee, and T. Simpson

ABSTRACT

A flowmeter has been developed for measuring flow velocity in hot slurries. The flowmeter works on an ultrasonic Doppler principle in which ultrasound is injected into the flowing fluid through the solid pipe wall. Isolating waveguides separate the hot pipe from conventional ultrasonic transducers. Special clamp-on high-temperature transducers also can be adapted to work well in this application. Typical flows in pilot plants were found to be laminar, giving rise to broad-band Doppler spectra. A special circuit based on a servomechanism sensor was devised to determine the frequency average of such a broad spectrum. The device was tested at different pilot plants. Slurries with particulates greater than 70 μm (0.003 in.) yielded good signals, but slurries with extremely fine particulates were unpredictable. Small bubbles can replace the coarse particles to provide a good signal if there are not too many. Successful operation with very fine particulate slurries may have been enhanced by the presence of microbubbles.

SUMMARY

The ultrasonic Doppler flowmeter measures the transport velocity of solid/liquid or liquid/gas-bubble slurries. High-temperature slurries can be measured using special standoff waveguides or specially designed high-temperature transducers.

Data indicate that for reliable flowmeter operation, particulates must be larger than ~50 ± 20 μm (if there are no bubbles). Small quantities of bubbles (estimated at <0.1% by volume) will enhance the Doppler signal, but large quantities (>10%) will prevent adequate penetration of the sound beam, ultimately making the meter respond to the flow near the wall only and giving misleading results.

Under field conditions, good operation was obtained when the necessary conditions were met, but when these conditions were not met, operation was unpredictable. Further study is required for a more precise definition of operating-condition limits in terms of pipe size, particle size, distribution, bubble content, bubble size, and liquid viscosity.

At low flow velocities, settling has been observed in horizontal lines for certain concentrations (35-50% by mass). When this occurs, low-velocity high-density flow is paralleled by a lower-concentration faster flow above it. If low-flow conditions are likely, flow measurement must be confined to vertical runs until ambiguities can be resolved by extensive research on flow separation or by flow separation measurement.

If the rheological properties of the fluid are not known, then the flow profile assumed for Newtonian fluids is invalid and an unknown correction factor introduces a significant calibration error. Two suggestions for dealing with this problem are outlined in Section 6--(1) multiple local velocity measurement to determine the profile empirically; and (2) forcing a limited flat profile at a constriction.

1. INTRODUCTION

Measurement of slurry flow is important in the control of coal-conversion plants. Conventional orifice-differential pressure instruments are limited in terms of operability, maintainability, accuracy, and reliability. Several alternative systems are under development concurrently at ANL.[1-7] This report concerns the design and performance of the ultrasonic Doppler flowmeter, which is in a more advanced stage[8,9] of development than other systems being investigated.

A description of the ANL Doppler flowmeter and a discussion of its design considerations are presented in Sec. 2. Section 3 is a discussion of the Doppler effect as it applies to development of the ANL flowmeter. Calibration and performance of the flowmeter are described in Secs. 4 and 5, respectively. The development needed to improve the flowmeter is discussed in Sec. 6, followed by a general discussion and conclusions in Sec. 7.

2. DESCRIPTION OF THE ANL DOPPLER FLOWMETER

2.1 PHYSICAL DESCRIPTION

The ANL Doppler flowmeter uses an ultrasonic signal, with an externally mounted transducer, injected obliquely into a slurry-filled pipe. Only the sound energy penetrates the pipe wall. A second transducer detects sound energy scattered by the particles (or bubbles) in the slurry. The scattered signal differs from the original signal in frequency by the Doppler shift:

$$f_d = \frac{2 f_t \cos \theta}{c} u, \qquad (1)$$

depending on the transmitted carrier frequency, f_t, of the injected signal, flow velocity u, sound velocity c, and the angle θ between the direction of the flow and the sound beam. The instrument output depends on the Doppler shift f_d.

Commercial Doppler ultrasonic flowmeters are marketed, but their performance has not been satisfactory in the typical environments of coal conversion plants. The system consists of the pipe conveying the slurry, transducers mounted on the pipe, and an electronics box in a convenient location--usually a control room--within ~500 ft of the flow sensors. The ANL Doppler flowmeter is shown in Fig. 1, and the basic operating principle in Fig. 2.

A quartz-crystal-controlled oscillator generates a signal that is amplified and converted to ultrasonic waves by the transmitting transducer mounted on the pipe in which the flow is measured.

A second transducer picks up the ultrasonic energy scattered by the slurry particles and converts this to an electric signal.

The electric signal is amplified by an amplifier (a few inches from the transducer) capable of driving a coaxial shielded 96-ohm cable.

The electronic circuit mixes this received signal with a portion of the transmitted signal in a double balanced mixer to produce a frequency difference signal, which is then analyzed further as to its frequency content to yield the desired flow information. The mixer effectively multiplies the transmitted and received signals: $2 \times \cos 2\pi f_t \times \cos 2\pi f_r t \equiv \cos 2\pi(f_t+f_r) t + \cos 2\pi(f_t-f_r)t$. The sum signal $\cos 2\pi(f_t + f_r)t$ is then filtered off.

2.2 DESIGN CONSIDERATIONS

ANL Doppler flowmeter development has addressed three specific problems encountered in the field:

The high temperature of the fluid,

The high viscosity of the fluid and consequent laminar or quasi-laminar flow conditions, and

Specific low-frequency noise problems.

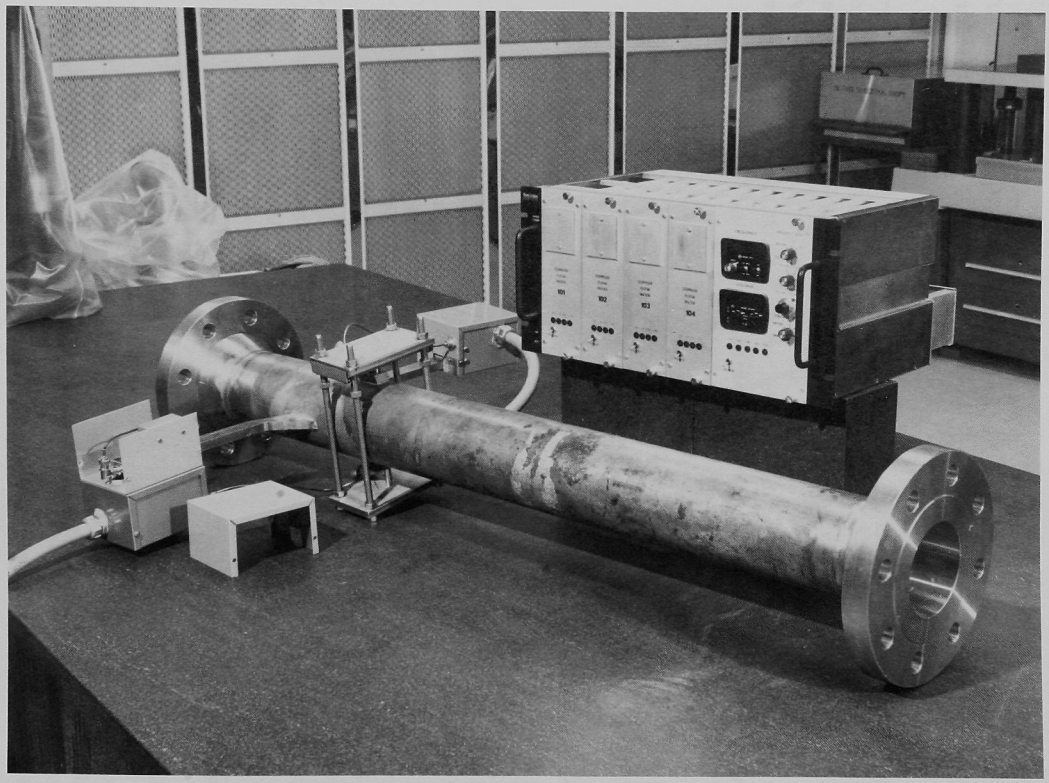

Fig. 1. ANL Doppler Flowmeter Showing a 4-in. Spoolpiece Before Installation on H-Coal Hydroclone Inlet. There are two stand-off wave guides as well as two clamped-on high temperature transducers. The four-channel electronic system with readout and test module can be seen behind the spoolpiece.

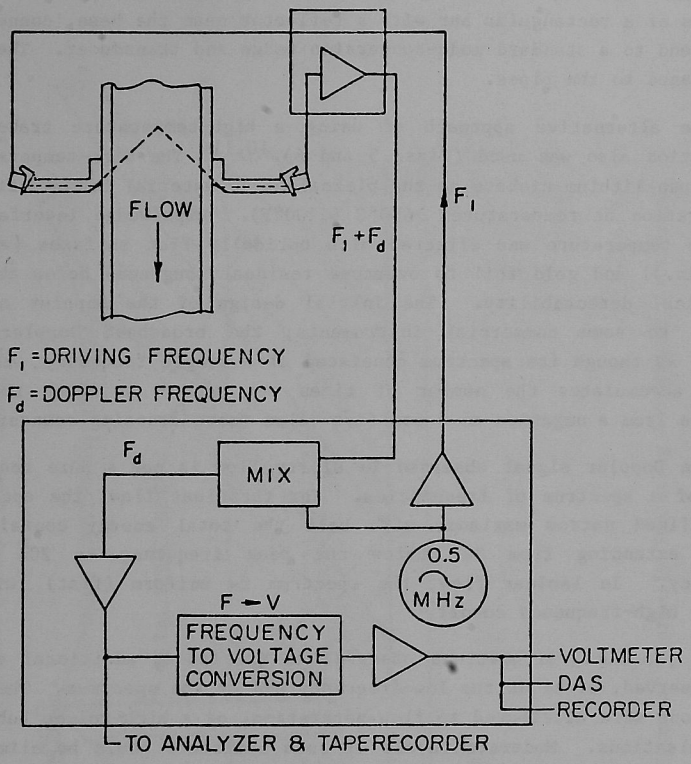

Fig. 2. Schematic of Transducer Installation and Signal-processing System.

Diverse thermally isolating acoustic waveguides were considered as a way of accommodating standard transducers for high-temperature flow systems (Fig. 3). The type of waveguide that has been built and tested (Fig. 4) consists of a rectangular bar with a reflector near the base, connected at the remote end to a standard mode-conversion wedge and transducer. The waveguides were brazed to the pipes.

The alternative approach of using a high-temperature transducer/wedge combination also was used (Figs. 5 and 6).[10,11] The high-temperature transducers use lithium niobate as the piezoelectric material because it is capable of operation at temperatures >650°C (1200°F). Pipe/wedge interface coupling at high temperature was effected with optically flat surfaces [within ~1 μm (40 μ in.)] and gold foil to overcome residual roughness below the threshold of optical detectability. The initial design of the Doppler analyzer was similar to some commercial instruments; the broadband Doppler signal is treated as though its spectrum consisted of a single frequency, and a counter simply accumulates the number of times per second in which the amplitude switches from a negative to a positive value (zero crossing counter).

The Doppler signal observed in slurry flow is not a pure tone, but consists of a spectrum of frequencies. For turbulent flow, the spectrum has a well-defined narrow maximum, with half the total energy contained in the region extending from 20% below the peak frequency to 20% above this frequency. In laminar flow, the spectrum is uniform (flat), with a well-defined high-frequency cutoff.

In practical situtations observed in the field, additional complexities were observed, often at the low-frequency end of the spectrum. The unexpected situations were attributed to flow separation, or a high-volume bubble flow or flow pulsations. Moderate levels of such artifacts could be eliminated with suitable filters. More details are given in Sec. 3.

These field observations led to the development of a more elaborate servomechanism filtered-signal follower to determine the "effective" Doppler frequency. The general principle of this design is discussed in Sec. 3.4, with details relegated to Appendix A.

Particular attention also is given to the special problem of operating multiple flowmeter units in the same plant (see Sec. 3.4.2). Individual electronic units were used for each pair of transducers; the concurrent use of several units in the same plant produced interference, due to beats between the carrier frequencies of individual units. Synchronization of the oscillators was the most convenient way to eliminate the problem.

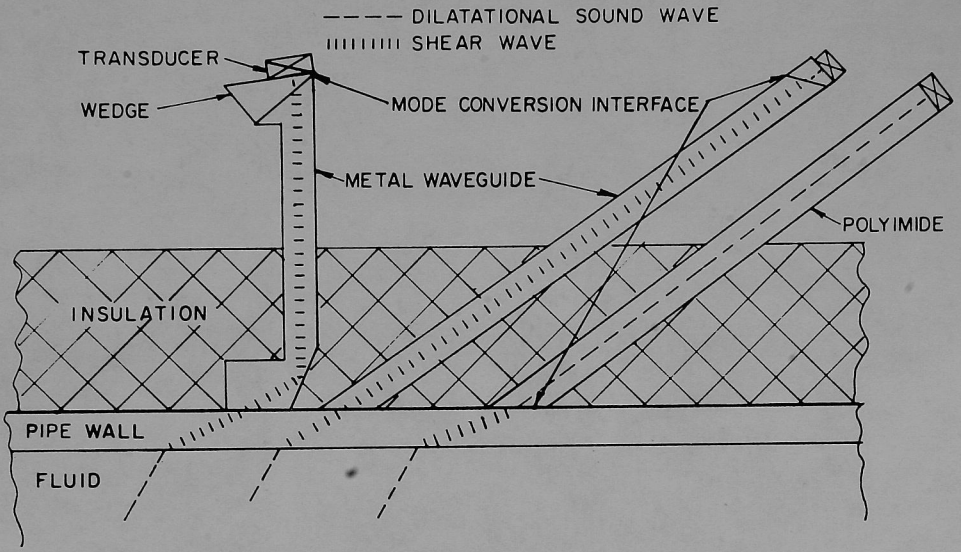

Fig. 3. Three Forms of Thermally Isolating Waveguides Considered.

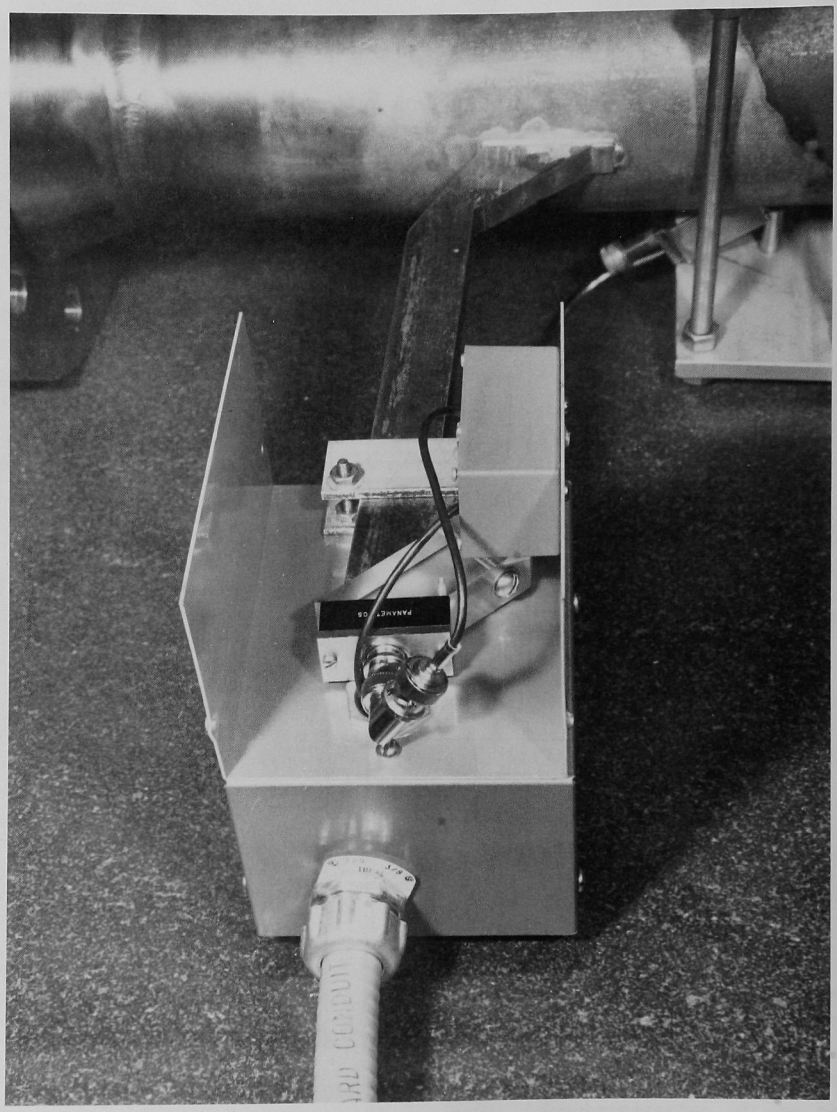

Fig. 4. Details of Waveguide Selected. Shown are the Lucite wedge and commercial transducer, and receiving preamplifier. Part of a high-temperature transducer is shown in the upper right corner.

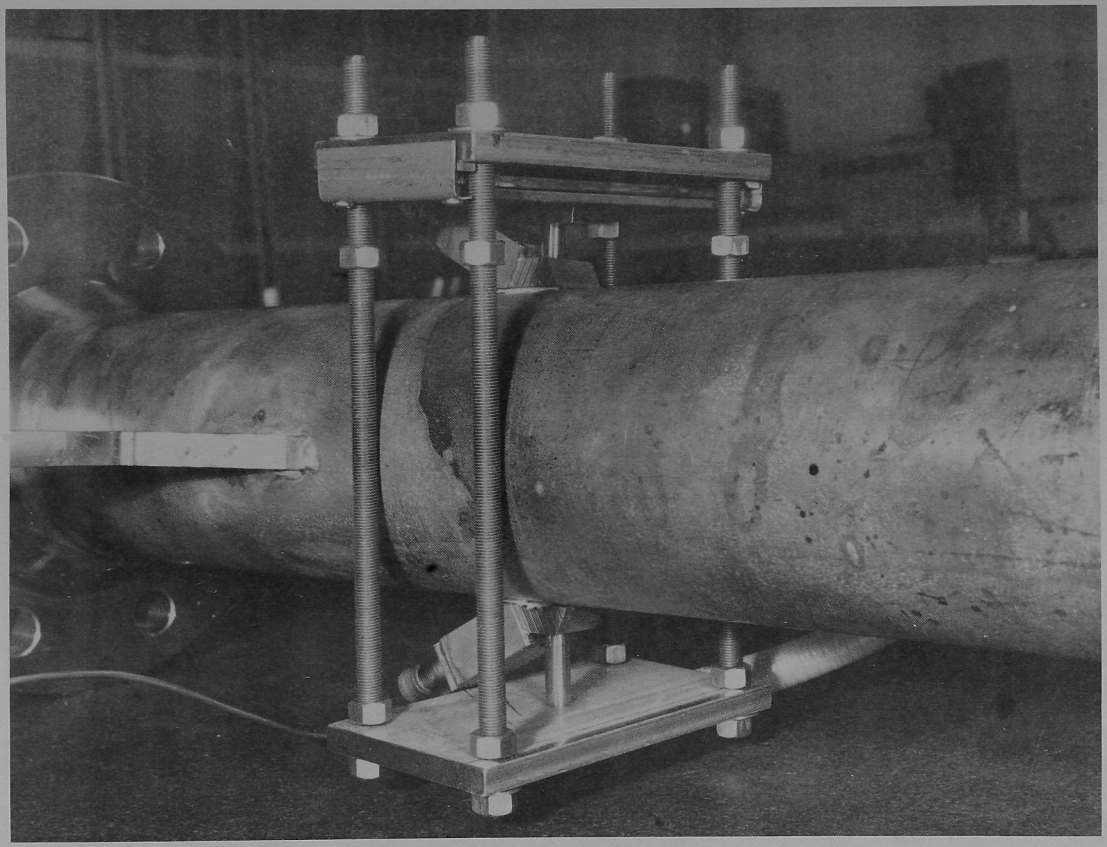

Fig. 5. High-temperature Transducer Clamped to 4-in. Pipe.

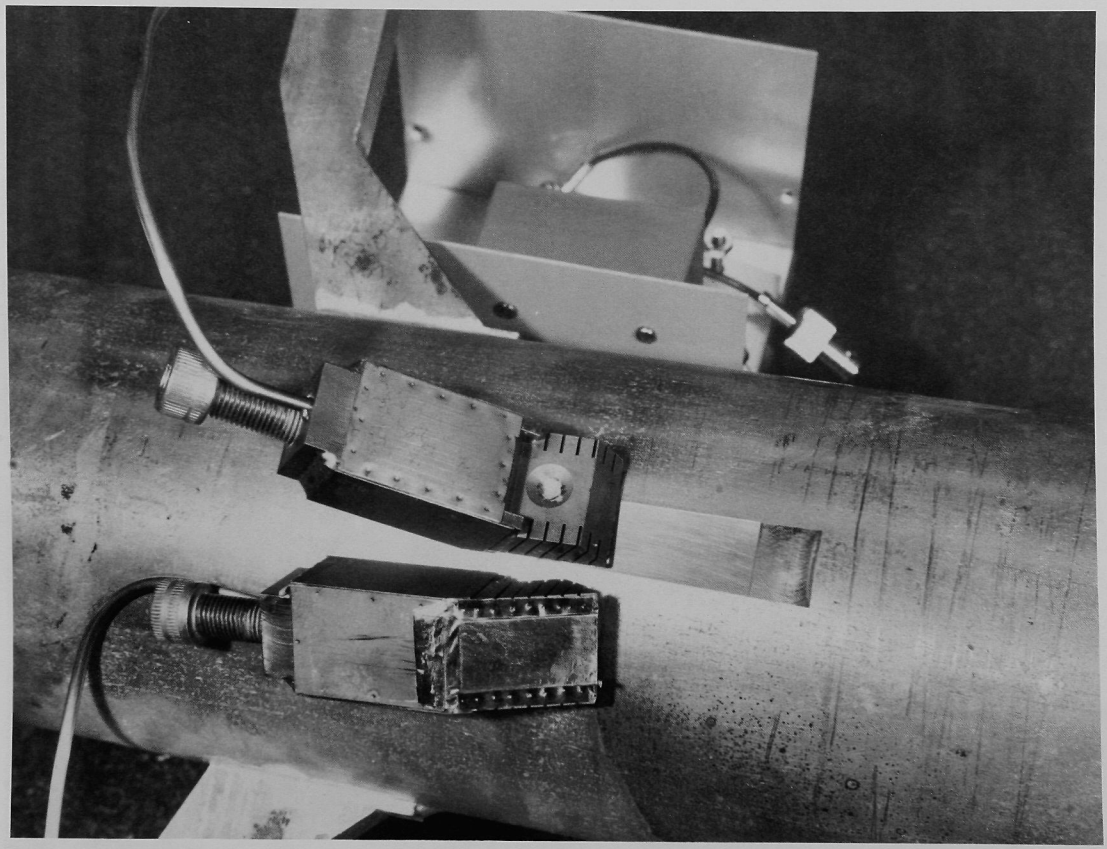

Fig. 6. Closeup of High-temperature Transducers.

The output of the ANL Doppler is given in two forms. A stream of pulses of 5V amplitude and 10 μs duration is generated such that the pulse repetition rate is proportional to the flow velocity being measured. Alternatively, 0-10V output is available, with a continuously adjustable relation of the output voltage to the flowrate. This permits setting any desired full-scale flow on a strip chart recorder. The flow velocity to pulse rate output was determined using flow in a 2-in. pipe feeding a weigh tank. The pulse rate output to voltage output is readily determined with a steady-state electronically generated pulse rate.

2.3 FLOWMETER SPECIFICATIONS

The ANL Doppler flowmeter consists of a flow channel and an electronic conversion unit yielding an output voltage proportional to flow velocity. In the version installed at the H-Coal Pilot Plant in Catlettsburg, KY, four flowmeters were installed in a single 19 in. rack of the NIM (nuclear instrument module) type together with a calibration and readout unit.

Each Doppler flowmeter electronic unit consists of a signal generator with a power amplifier, a mixer receiver, and a signal interpreter. The output is in the form of a pulse repetition rate or a voltage proportional to flow.

Specific parameters of the flowmeter are discussed below.

Power

115 V, 60 Hz, 100 W.

Operating Frequency

The operating frequency of unit serial number 101 is plug-selectable by a quartz crystal (currently, 1 MHz).

For Units S/N 102 and 103, input frequency is from the adjacent unit.

Unit S/N 104 contains a frequency divider which, when driven by 1 MHz, puts out 0.5 MHz (see Table 1 for operation options). The coupling or dividing circuit in units 102, 103 and 104 can be replaced with a quartz crystal to make them master units like unit 101.

Receiver

The remote preamplifier operates on 5 V dc carried with the signal in the RG62/U cable. Preamplifier gain is ~300.

Table 1. Operating Frequency Selection by Unit Placement

Unit placement 1	101*	102	103	104†
Operating frequency, kHz	1000	1000	1000	500
Unit placement 2	101*	102	104†	103
Operating frequency, kHz	1000	1000	500	500
Unit placement 3	101*	104†	102	103
Operating frequency, kHz	1000	500	500	500

*Master unit.
†Fitted with a divide-by-2 unit.

Signal Conditioner

The mixer puts out a Doppler (difference) signal. There is a high-pass filter; the low-frequency cutoff is adjustable from 5 to 50 Hz, automatic gain control signals are automatically adjusted to 1.3 V rms into the analyzer circuit.

Output

Pulse repetition rate: Output pulses of 5 V (up to 2 ma) and 2 μs duration. The repetition rate is proportional to the "average" Doppler frequency. The proportionality constant is given on a separate calibration chart for each unit. Nominally, it is 100 times the "average" Doppler frequency. Output range is up to 200,000 Hz. This output is convenient for automatic digital data acquisition systems.

Voltage

The output voltage is proportional to the pulse repetition rate (described above). The constant is continuously adjustable with a ten-turn screwdriver adjustable potentiometer and four range selector switches. Output voltage is 10 V full scale; it can be adjusted to correspond to any output repetition rate between ~10,000 and 200,000 Hz. This output is useful for direct recording on strip charts.

Time Constant

Two output voltages are provided--a "fast" output with a 6-s integration time and a "slow" output with a 60-s integration time. The slow output also has a 10 V Zener diode overvoltage limiter. The fast output can reach +14.5 V.

Tranducers

Standoff waveguides with 22.5° reflectors at the base and mode conversion lucite wedge at the remote end are coupled to a commercial NDT rectangular transducer with a 13 x 25 mm (1/2 in. x 1 in.) piezoelectric element. The combination radiates (and receives) sonic shear waves into the pipe at an angle of 45° with the pipe axis. These shear waves are subsequently transmitted through mode conversion at the inside pipe wall as longitudinal waves in the slurry. Standard 0.5-MHz or 1-MHz transducers are suitable, depending on the application, and should match the frequency of the power source transducer to which they are connected (see Sec. 3).

Readout Monitor

The output of each flowmeter can be read on the frequency meter and voltmeter provided on an additional (double-width) module in the same 19-in. rack NIM crate. A switch with numbers 1-4 permits reading the output of each unit counting from the left. Output repetition rate is read on the frequency meter (upper meter) and output voltage is read on the (lower) voltmeter.

Calibrate Signal

A white noise signal with precisely defined high-frequency cutoff (better than 80 dB/octave) can be injected into the analysis circuit instead of the Doppler signal under test. To determine the filter cutoff frequency, the frequency meter selector switch is set to "filter." The frequency read on the meter is now 100 times the cutoff frequency of the test filter.

To calibrate a unit with the test signal, the DIP switch behind the front panel access cover is used. Switch 8 on (up), 7 off (down) is for measurement and 8 off, 7 on for calibration with the electrical noise test signal. Units 101, 105, and 111 were revised to use a PC board switch instead of switches 7 and 8. This reduces noise but requires unplugging the unit and removing one cover to operate the switch.

Slurries

Operation requires scatterers in the fluid. Particulates >50 (± 20) μm are satisfactory even up to 50% concentration. Somewhat smaller particles can be used at modest concentrations. Microbubbles are equally useful scatterers, but should not exceed a fractional percent by volume, depending on bubble size; otherwise there is excessive attenuation.

3. THE DOPPLER SIGNAL

The ease of demonstrating the Doppler effect permits its inclusion at this point.

Sound waves propagating with sonic velocity c through a fluid are scattered by particles in the fluid moving with a velocity u and direction θ_1 toward the sound transmitter scattering sound into the receiver in direction θ_2. Consider two successive peaks of the sound wave. The peaks are separated by the time of one period t (equal to the reciprocal of the frequency f: t = 1/f). During the time interval, t, the distance between the particle and the tranmitter has been reduced by an amount tu·cos θ_1 and similarly the distance to the receiver is reduced by tu·cos θ_2 so that the distance the second peak travels to the receiver is shorter by the distance tu cos θ_1 + tu cos θ_2; or, in the special case $\theta_1 = \theta_2 = \theta$, the distance to be traveled is reduced by 2 tu cos θ. The sound wave traveling with velocity c traverses this distance in time 2 tu cos θ/c. Consequently, the arrival of the successive peaks of the sound wave to the receiver is t - 2(t u/c) cos θ. The reciprocal of this time interval is the frequency of arrival of the sound wave. Neglecting the higher-order terms in the expansion of the reciprocal, the received frequency f_r becomes

$$f_r = \frac{1}{t[1 - 2\ (u/c)\ \cos\theta]} \triangleq f_t[1 + 2\ (u/c)\ \cos\theta]. \qquad (2)$$

Hence, $f_d = f_r - f_t = 2\ f_t(u/c)\ \cos\theta$. (3)

3.1 EXTERNAL TRANSDUCERS

There is an additional observation of interest at this point with respect to the injection of sound waves through the wall of the pipe. The sound waves refract at the wall/liquid interface. According to Snell's Law, the cosine of the angle θ_f of the beam in the fluid will relate to the corresponding cosine of the angle in the pipe wall θ_p in the ratio of the relative sound velocities in the fluid and the pipe:

$$c_f/\cos\theta_f = c_f/\cos\theta_p. \qquad (4)$$

Consequently, it is not necessary to know the sound velocity of the fluid. If we know the sound velocity in the pipe wall and the angle of the beam in the wall, we are assured that the ratio cosθ/c will be the same in the fluid and the wall. Thus, we can substitute the sound velocity c_p and sound direction angle θ_p in the pipe wall in the basic equation (1), and rest assured that the calibration factor will not change with the velocity of sound in the fluid.

The same argument applies by further translation to mode conversion plastic wedges placed on the outside of a pipe. Again, sound velocity c_w in the wedges at angle with the pipe axis θ_w yields

$$c_w/\cos\theta_w = c_p/\cos\theta_p = c_f/\cos\theta_f. \qquad (5)$$

3.2 OBSERVED DOPPLER SIGNALS

The formula given above for the relation between the Doppler signal and the flow velocity does not imply that the Doppler signal is a pure tone. The particles do not all travel at the same speed and the sound beams have only limited collimation so that the angle is not exactly the same for all scattered sound waves accepted by the receiver. Consequently, the received signal consists of a range of frequencies that can be plotted as a spectrum.

Observations of the flow of different fluids have shown that the spectrum of the Doppler signal varies with the conditions of the setup, depending on the velocity distribution of the particles and the interaction of the sound beam with the flow in the pipe.

Let us first look at some observed spectra (Figs. 7-9). These spectra show the amplitude of each frequency component on a logarithmic scale as a function of the Doppler frequency f_d, plotted on a linear scale horizontally. The vertical scale is in decibels: $20 \log_{10} V/V_o$, where V/V_o is the relative value of the amplitude of each frequency component referenced to an arbitrary level V_o, which is not of interest in the examination of spectrum shape. Absolute levels are not of interest, as only the "average" frequency of the spectrum is required to determine flow. By choosing the logarithmic decibel scale, the shape of the spectrum is unaffected by changes of gain, transmitter power, incidental conversion losses, etc., but will simply result in a parallel vertical displacement of the spectrum. The absolute base line or zero level of the ordinate is therefore arbitrary and only the spacing is important.

3.2.1 Preliminary Laboratory Flow Loop

The first spectrum (Fig. 7) was obtained in a loop put together for initial tests using coal and water. The coal concentration was about 10% by mass and the viscosity was reasonably low (it was not thought important at the time to measure it). The spectra obtained for three different flow rates are shown. Each spectrum is seen to exhibit a pronounced maximum with frequencies higher and lower having significantly lower amplitudes. About half the energy (3 dB points) is within about half an octave--that is, the highest to the lowest frequency of the central 50% energy region is in the ratio $\sqrt{2}$:1.

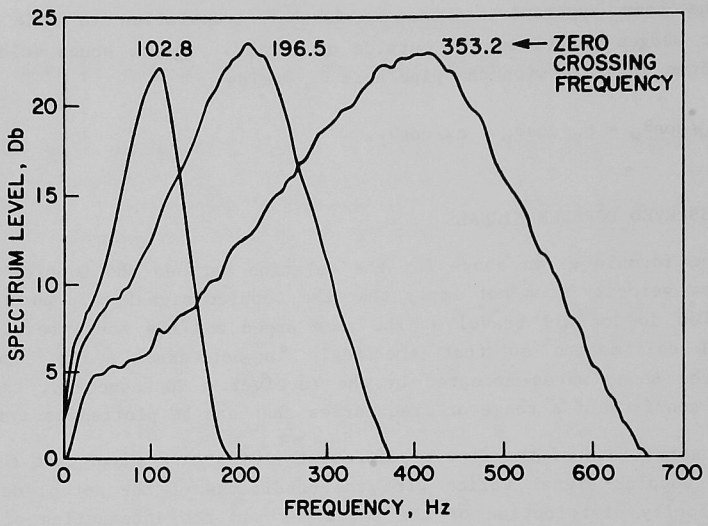

Fig. 7. Doppler-shift Signal Spectrum for Turbulent Flow at Various Flow Velocities. The numbers give the counts of an "effective frequency" meter.

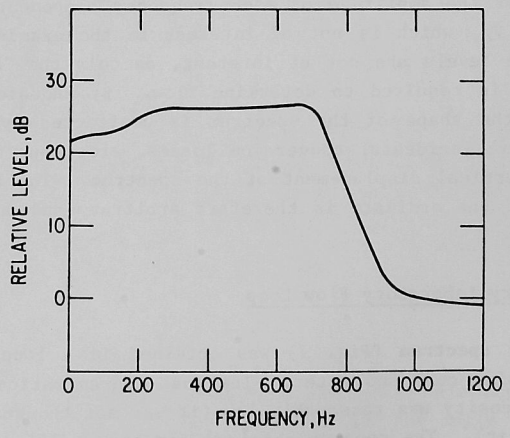

Fig. 8. Acoustic Doppler Flowmeter Spectrum at 60 wt% Coal Concentration and 1.2 m/s Slurry Velocity.

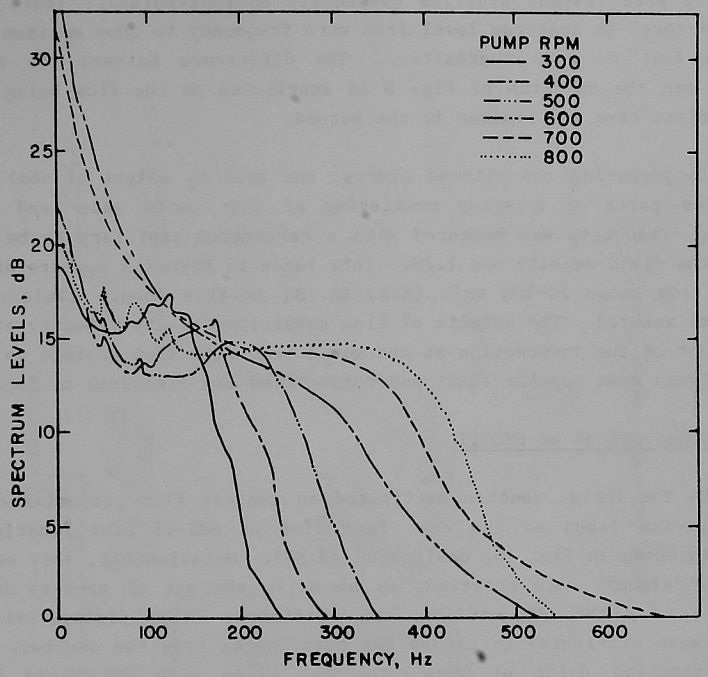

Fig. 9. Doppler-shift Signal Spectrum for Laminar Flow and Various Pump Speeds at SRC-II.

3.2.2 Modified Loop

Quite a different spectrum is seen in Fig. 8, obtained in a similar loop with more viscous slurries (viscosity 60 centipoise). There is only a small increase in spectrum level from zero frequency to some maximum value and a rapid fall to zero thereafter. The difference between the spectra of Figs. 7 and the spectrum of Fig. 8 is attributed to the flow being turbulent in the first case and laminar in the second.

In preparing the viscous slurry, one part by weight of coal was mixed with nine parts of a syrup consisting of four parts water and six parts sucrose. Viscosity was measured with a calibrated capillary to be 60 centipoise; the fluid density was 1.29. This leads to Reynolds numbers of 220-2200 in the flow range 20-200 cm/s (8-80 in./s) in this loop. Laminar flow was therefore assured. The effects of flow conditions on the velocity profile and the effect of the interaction at the sound beam with flow profile on the relation between mean Doppler shift and volume flow are discussed in Sec. 3.3.

3.2.3 Observations at SRC-II

In the field, spectra attributed to laminar flow predominate. Fig. 9 shows spectra taken on the coal feed line at SRC-II (the location of the sensor is shown in Fig. 10, designated as M1). Occasionally, very strong low-frequency signals were observed, as shown in the set of spectra in Fig. 9, especially for the 600 and 700 rpm condition. These strong low-frequency signals were attributed to excess gas overflowing from the snubber. From the plant operation point of view, the gas mixed with the fluid was quite negligible compared with the large quantities of hydrogen injected farther downstream. However, these additional bubble sound scatterers changed the character of the spectrum significantly. An adjustable high-pass filter was added to the design of the flowmeter to eliminate the detrimental effect of this low-frequency noise.

3.2.4 Contamination With Gas

It should also be noted that for very high gas flow rates, the Doppler spectrum was completely masked. This is shown using a different type of spectrum analyzer. Two spectra are shown in Fig. 11 with and without gas flow. In this case the raw spectrum (f_r) as received by the receiving transducer is shown directly. The main central spike is at the transmitted frequency f_t, in this case 500 kHz. At a spectrum level 60 dB below the central maximum, a fairly flat spectrum is seen to the left of the central maximum with a sharp cutoff at $f_t - f_d = 499{,}700$ Hz.

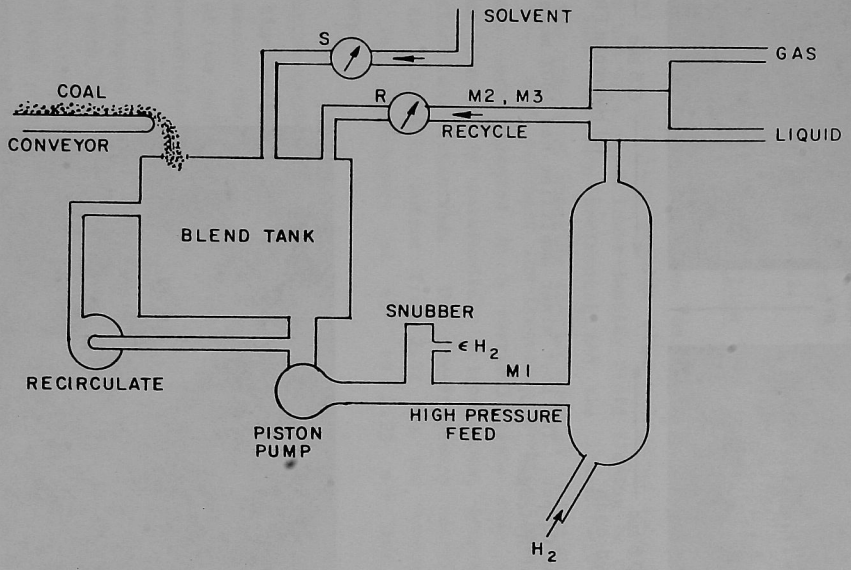

Fig. 10. Schematic of Flowmeter Location at SRC-II.

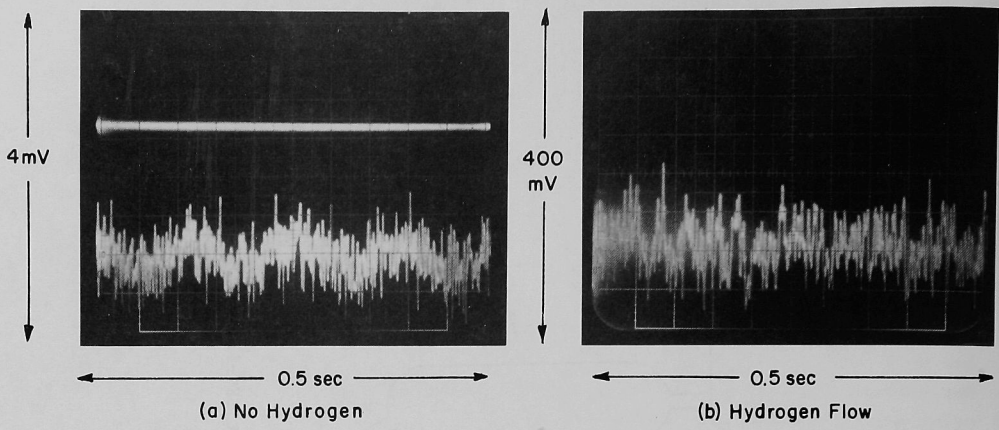

Signal from Mixer Output. The post mixer amplifier had 100X more gain in the absence of hydrogen flow.

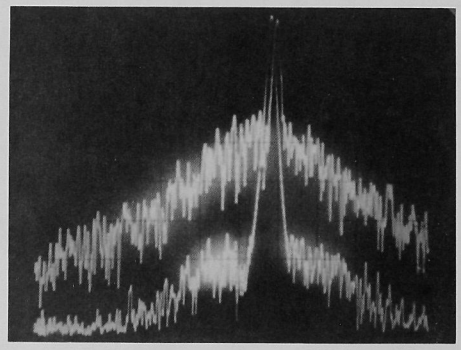

Fig. 11. Spectrum at Receiving Transducer. For the upper curve, there was a hydrogen flow of ~1 g/s (8 lb/h); for the lower curve hydrogen flow was stopped.

The second spectrum, superimposed on the first, was taken with gas flow. The central maximum is essentially the same intensity, but the side bands are about 30 dB more intense. However, in this case a monotonic decrease in intensity is observed, without the sharp break shown in the lower curve. This case of high gas flow (~10±5% by volume) produced a very large Doppler signal (30 dB higher, i.e., 1000 times the energy) than the slurry particles did; however, the shape of this spectrum could not be related in any simple way to flow rate. Spectra of the difference frequency, f_d, analogous to Figs. 7-9 are shown in Fig. 12.

3.2.5 Settling in a Horizontal Line

Low-frequency disturbances on a flow loop, shown in Fig. 13, were attributed to a settling problem with a high-density fluid flowing in the bottom of the pipe and a lower-density fluid flowing in the upper region. The pipe in this case was horizontal and the transducers were in a vertical plane. The effect of changing the location of the transducers also is shown in Fig. 13. Much stronger low-frequency contributions were noted when the transducers were oriented in a vertical plane than when they were in a horizontal plane. At intermediate orientations, intermediate low-frequency contributions were observed. The low-frequency contribution in this case changed the flowmeter output from 2.92 m/s for horizontal transducers to 2.63 m/s for transducers at 45° to 2.06 m/s for vertically mounted transducers.

Corroborating evidence was obtained with an acoustic cross-correlation transit time meter placed immediately adjacent to the Doppler meter. This meter measures the cross-correlation function of the fluctuations of acoustic signals of two pairs of sound beams 12.7 cm (5 in.) apart. Whereas normally the cross-correlation exhibits a single strong peak for the flow condition shown here, two distinct peaks are observed at 30.2 and 258.9 ms (Fig. 14); these correspond to velocities of 4.2 m/s and 0.49 m/s. The average velocity measured with the weigh tank calibration was 2.9 m/s. The coal concentration in the oil slurry for this particular observation was 43% by weight. Similar slightly less pronounced "settling" was observed at 49% concentration. At lower concentration (<35%) and at (higher) 60% concentration, this separation was not observed.

3.2.6 Observations at SRC-I

A low-frequency spectrum disturbance also was noted in the spectra observed in the feed line at SRC-I (Fig. 15). When first installed, the flowmeter was set up with a high-pass filter set to 25 Hz; it worked well as the flow was increased from 750 to 1000 lb/hr, but the output dropped when the [illegible] was increased to 1500 lb/hr. Operation of the flowmeter was

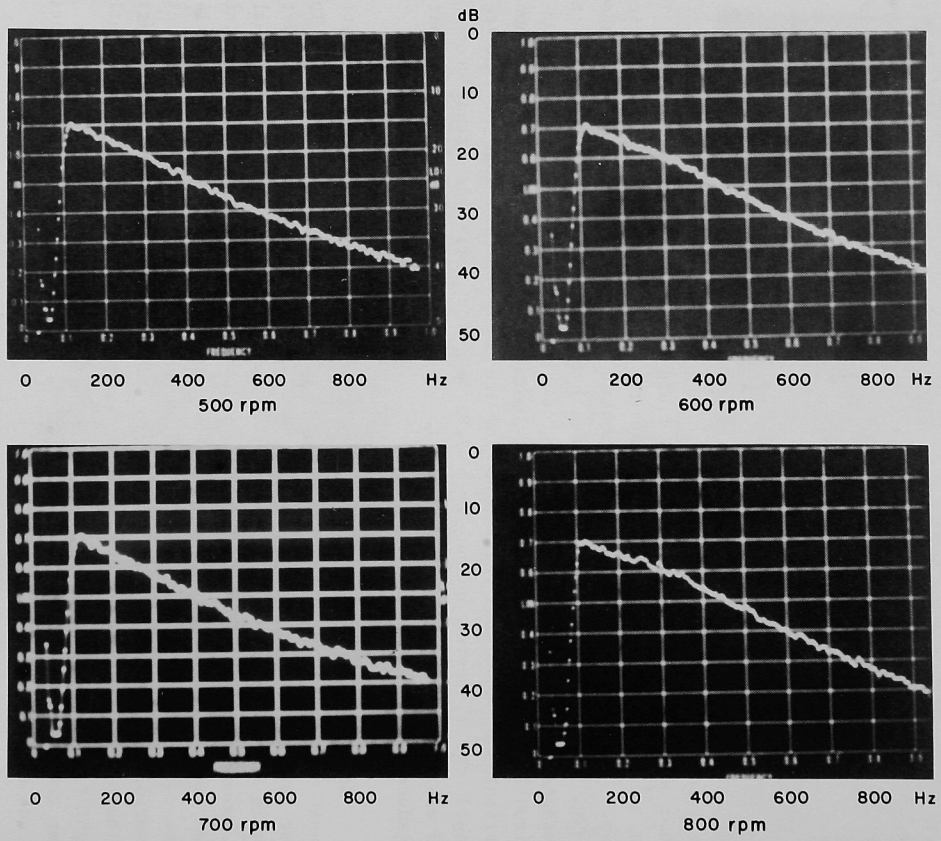

Fig. 12. Spectra from Doppler Flowmeter for Different Flow Rates of Coal Slurry with Gas Bubbles.

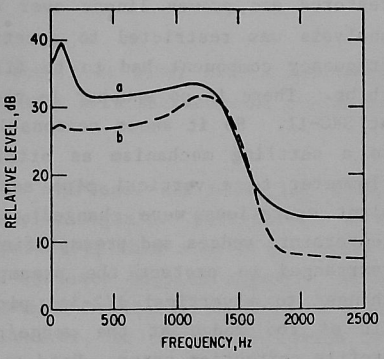

Fig. 13

Doppler Spectrum from a Horizontal Line on the SLFTF Loop at 40% Coal Concentration; Transducer Orientation: (a) Vertical Plane; (b) Horizontal Plane.

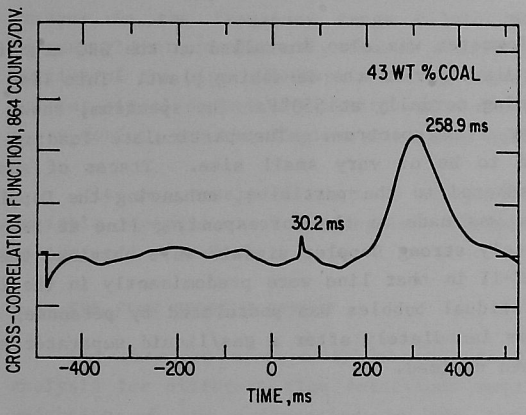

Fig. 14

Cross-correlation Function Obtained with Vertically Oriented Acoustic Transducers during Phase Separation.

Fig. 15

Doppler Spectrum from Coal Feed at SRC-I--880 lb/hr (35.8 cm/s, 1.17 ft/s). The built-in high pass filter will cut off the low-frequency component. (The 60 Hz and 180 Hz HUM components appear only during this test of the low level signal, picked up by the probe.)

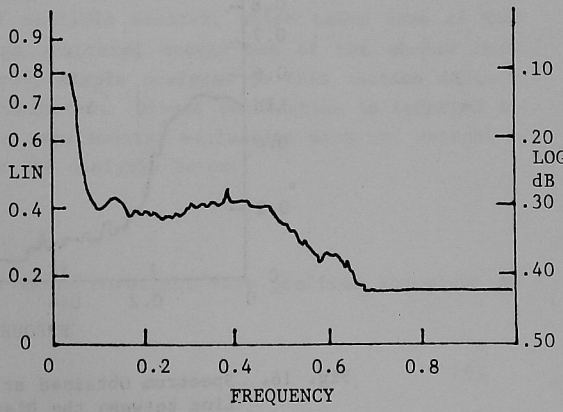

restored and proven linear over the 700-1500 lb/hr range when the flowmeter analysis was restricted to spectral components above 40 Hz. A strong low-frequency component had to be filtered off when the flow rate exceeded 1000 lb/hr. There is no snubber in the line at SRC-I corresponding to the snubber at SRC-II. So it seems reasonable to attribute the low-frequency components to a settling mechanism as attributed in the flow loop. Transfer of the flowmeter to a vertical pipe section would be appropriate. Unfortunately, plant operations were changed to reach higher temperatures, and the room-temperature wedges and preamplifier were damaged. The system was subsequently rearranged to protect the preamplifier from excess heat and the location changed to a vertical 1/2-in. pipe (from the horizontal 3/4-in.). The poor fit of the wedge at the wedge/pipe interface will lead to an additional profile correction error. Data to be supplied by plant operators.

On the SRC-I plant a flowmeter was also installed on the SRC transfer line taking the fluid from the dissolver to the de-ashing plant. This line is 19 mm (3/4 in., Sch. 80), running normally at 550°F. The spectrum, shown in Fig. 16, is the normal laminar flow spectrum. The particulate loading is predominantly ash and believed to be of very small size. Traces of small bubbles are believed to have adhered to the particles, enhancing the Doppler signal. A similar observation was made on the corresponding line at SRC-II (Fig. 10 position M2). Adequately strong Doppler signals were obtained there also. Particulate sizes at SRC-II in that line were predominantly in the 2-5 μm range. The existence of residual bubbles was postulated by personnel at SRC-II because this line follows immediately after a gas/liquid separator and perfect separation has never been claimed.

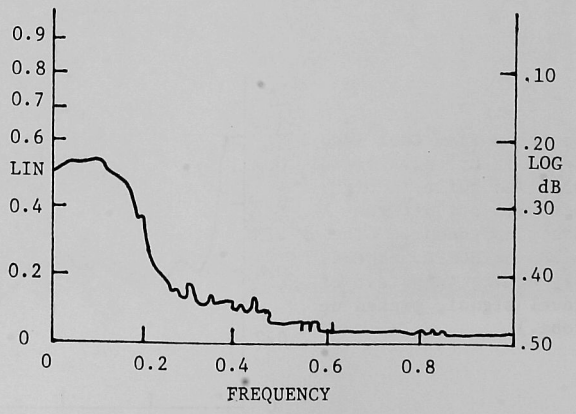

Fig. 16. Spectrum Obtained at SRC-I Plant on 550°F Line between the Dissolver and the De-ashing Plant. The incident frequency was 1MHz.

3.2.7 Observation at H-Coal

At H-Coal results similar to the result at other plants were obtained for the slurry feed line transporting a slurry with particulates predominantly 70 μm in diameter.

Other flowmeters on the hydroclone overhead, the ebulating flow, and the hydroclone feed yielded inadequate Doppler signals. Particulates in these lines were reported to be 10-20 μm. Apparently, this size is too small in a high-concentration slurry to produce an adequate Doppler signal. At lower concentrations it is possible to adjust the transmitted frequency to a higher value to obtain adequate scattering. However, at the concentration in the three lines assayed at H-Coal (other than the slurry feed), extensive investigations in the frequency range 0.3-10 MHz failed to show any operating frequency that consistently showed a strong Doppler signal from the central portion of the pipe. Without a strong signal from the center of the pipe, the Doppler signal depends on particle size distribution and concentration as well as on motion, and the simple system used does not yield unambiguous flow data.

It was concluded that 20 μm particulates are too small to permit reliable operation of a Doppler flowmeter in the concentration range encountered at H-Coal.

3.3 THE FLOW PROFILE EFFECT

The observed spectra illustrated in the preceding section showed that analysis for different flow conditions requires attention to ensure that the weighting of the frequencies in the received signal corresponds to the weighting of the flow in the pipe. In this section, some of the interactions of the sound beam with the various flow profiles are considered. Not considered here is the effect of multiple scatter, which takes some of the beam into shadow zones and brings scattered energy out of the shadow zone toward the receiver. The relatively simple analyses in this section delimit the range of correction to be anticipated. Direct calibration is reported in Sec. 4. The repeatability of this experimental evaluation does not warrant a more detailed explanation of it in the analysis below.

3.3.1 Turbulent Flow

In typical fluid mechanics texts turbulent flow profiles are given in the form

$$u_r(r) = u_m(1 - r/r_o)^{\alpha} \qquad (6)$$

in terms of the maximum or centerline flow u_m and the pipe radius r_o. The exponent α varies from ~ 0.17 for Reynolds numbers just above the transition turbulence (Re = 3000) to a value close to 0.1 at Reynolds numbers above 1,000,000.

By interrogating the pipe with a sonic beam that does not fill the pipe completely uniformly, the measured velocity will be biased in favor of those regions in which the sound beam is more intense. Consider as an extreme example a very thin sound beam in a diametrical plane. The average velocity along the sound beam will be given by

$$\bar{u}_{dia} = \int_o^{r_o} u_m(1 - r/r_o)^{\alpha}\, dr / \int_o^{r_o} dr, \tag{7}$$

whereas the actual average velocity, $\bar{u}_s$ (volume flow $\dot{Q}$ divided by cross-section S), is given by

$$\bar{u}_S = \frac{\dot{Q}}{S} = \int_o^{r_o} u_m(1 - r/r_o)^{\alpha}\, r\,dr / \int_o^{r_o} r\,dr. \tag{8}$$

The ratio of these two quantities is $1/(1 + \alpha/2)$. The Doppler flowmeter overestimates the flow under turbulent conditions by 6-10%.

3.3.2 Laminar Newtonian Flow

The flow profiles for laminar flow of a Newtonian fluid (shear stress τ proportional to shear rate s') is given by

$$u(r) = u_m(1 - r^2/r_o^2)\ . \tag{9}$$

By simple integration, this yields

$$\overline{u_s} = u_m/2. \tag{10}$$

We also calculate the average velocity along a narrow diametral pencil

$$\overline{\overline{u_{dia}}} = \frac{1}{r}\int_o^{r_o} u(r)\, dr; \tag{11}$$

integrating yields

$$\overline{u_{dia}} = 2u_m/3 \ . \tag{12}$$

Hence,

$$\overline{u_{dia}} = 4\ \bar{u}_s/3 \ . \tag{13}$$

3.3.3 Laminar Pseudoplastic (Power Law) Flow

Certain slurries were investigated showing a non-Newtonian behavior yielding a power law for the stress-shear rate (τ, s') relationship

$$\tau = K\,(s')^n \ . \tag{14}$$

This relationship leads to a profile of the form

$$u(r) = u_m\,[1 - (r/r_o)^{(1+n)/n}] \tag{15}$$

(yielding the Newtonian profile for n=1).

This form is readily integrated:

$$\bar{u}_s/u_m = (1+n)/(1+3n) \tag{16}$$

and

$$\bar{u}_{dia}/u_m = (1+n)/(1+2n) \ . \tag{17}$$

Hence,

$$\bar{u}_s/\bar{u}_{dia} = (1+2n)/(1+3n) \ . \tag{18}$$

The limiting case n = 1 describes a Newtonian fluid and Eq. 18 assumes the same value as Eq. 13.

Further, notice that small values of n yield a flattened profile superficially more like the profile for turbulent flow. Also, $\bar{u}_s/\overline{u_{dia}}$ approaches the value calculated for turbulent flow; specifically, the value of $\bar{u}_s/\overline{u_{dia}}$ is 0.93 for turbulent flow at α = 0.14 and for pseudoplastic laminar flow when n = 0.08.

3.4 DOPPLER FLOWMETER DEVELOPMENT

The ANL Doppler flowmeter and its operating principle are described briefly in Section 2.1; the electronics system is described in Appendix A. The operating principle is summarized here to aid understanding of the results reported.

The instrument electronics contains circuit components consisting of:

A quartz-controlled oscillator and power amplifier to generate the signal (in multiple-unit operation, synchronization between units is needed, as discussed in Sec. 3.5),

A mixer giving the difference frequency signal between the received signal and the local oscillator,

A signal conditioning filter (high pass),

Automatic gain control, and

A signal analyzer giving a voltage output proportional to the Doppler frequency.

A brief explanation of the analyzer is important for an understanding of the quantity measured.

The earliest analyzer used a simple Schmidt trigger to generate a square wave having zero crossings coincident with the Doppler signal. The square wave was counted or converted to voltage with a frequency-to-voltage converter. Problems were encountered when very low-frequency signals were observed on the lines at SRC-II. Subsequently, signals were analyzed with a fast Fourier transform (FFT) analyzer; flat spectra very different from those observed on the laboratory loop were observed. Occasionally, very intense low frequencies also were seen. The flat spectrum is a characteristic of laminar flow. The intense low frequency was later recognized as caused by hydrogen bubbles spilling over from a depulser downstream of the piston compressor. Similar low-frequency components due to other causes were observed at SRC-I and on another oil/coal loop at ANL.

This type of behavior, as shown in Fig. 9 when the pumps were running at 600 and 700 rpm, is seen to have increased the low-frequency intensity about 15 dB. It was later found that this occurred when the gas flow into the snubber was spilled into the line. With further increase in gas flow the intensity of this low-frequency signal would increase an additional 15 dB and completely obliterate the portion of the signal used to measure flow rate.

The correlation of gas flow and Doppler signal was established beyond resonable doubt by stopping and starting the gas flow and observing the response of this very intense low-frequency signal during the gas flow.

The presence of gas bubbles adds to the scattering produced by the particles in the fluid. When the scatterers occupy a significant volume fraction (more than 10%), scattering near the surface prevents penetration of the sound beam to the middle of the pipe. Near the wall of the pipe the flow velocity is small and so only this low velocity (low-frequency Doppler) is detected.

The upper cutoff frequency of the flat spectrum was related to flow by correlating it with pump rpm; ultimately the relation was derived theoretically. To interpret this type of Doppler spectrum, the spectrum to voltage conversion was accomplished by servomechanisms (Fig. 17):

The signal was amplified to 1 V rms, using automatic gain control; a filter removes signals below a preset cutoff frequency (adjustable, 5-40 Hz) to eliminate the extraneous low-frequency components mentioned, and a second automatic gain control amplifier brings the signal up to 1.5 V.

The "average" frequency of the amplified signal is determined by passing it through an electronic low-pass filter (R5609) that passes half the signal put into it by cutting off the high frequencies--the cutoff frequency f_1 of this filter is controlled by a pulse repetition rate f_o with a frequency 100 times the filter cutoff.

The filtered signal is squared and averaged and compared with half the squared and averaged signal put into the filter; the departure of this ratio from unity is amplified and, by means of a voltage-to-frequency converter [VFC32], converted to the pulse repetition rate controlling the R5609 filter cutoff frequency.

Thus the cutoff frequency of this filter is servo-controlled to contain half the original signal and can be regarded as the weighted average frequency of the band. This cutoff frequency is equal to 1/100th of the pulse repetition rate controlling the filter, which in turn is precisely proportional to the voltage driving the voltage to frequency converter. Range settings are provided with switch selected capacitors and a potentiometer to vary the ratio. Details of the systems are given in Appendix A.

In Appendix A, two circuits are given. In the first one, the ratio of the signal filtered by the servo-controlled R5609 to the unfiltered signal was chosen to be 0.68 instead of 0.5 as described above. The original idea had

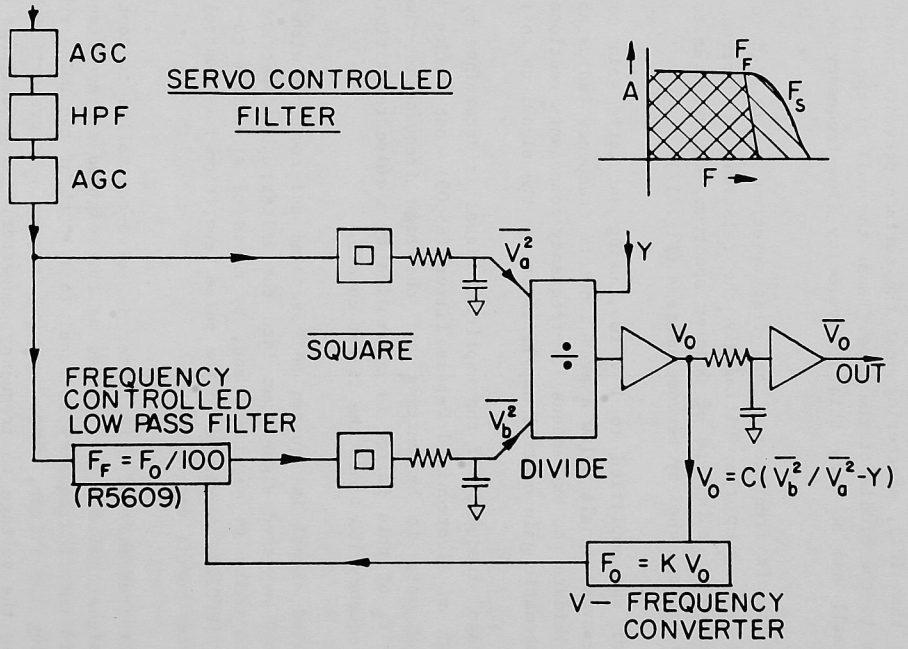

Fig. 17. Servomechanism System for Generating the Output Repetition Rate Proportional to the Effective Doppler Frequency.

been to locate a fixed fraction of a flat spectrum and the fraction 0.68 was entirely arbitrary. The change to 0.5 was made with the realization that a location of the effective centroid of the spectrum should yield a system giving a velocity average independent of spectrum shape, thus making the meter respond accurately to both turbulent and laminar flow.

The assumptions implicit in the above argument is a uniform coverage of the pipe with sound energy and a negligible elimination of the spectrum by the low-cut (high-pass) filter used to permit operation with spurious excessive low-frequency energy. This filter is to be considered an interim expedient to permit operation where normal operation would not have been otherwise possible. Ultimately the filter needs to be eliminated in order to restore rangeability of the meter and linearity at the low flow rates. This would be accomplished by eliminating the problem in the first place. In the case of SRC-II it would mean coordinating the meter with intermittent snubber overflow. The snubber would receive extra gas in bursts and during the overflow periods the flowmeter would be ignored. Similarly, the best current information for the need of the filter at SRC-I would be avoided if the meter were mounted on a vertical section of the flow system.

3.5 MULTIPLE UNIT OPERATION

Four flowmeters were mounted in a single rack together with a calibration generator (Fig. 1). The Doppler signal showed strong beat frequency signals at the difference frequency of the individual oscillators. After we failed to isolate or shield the units sufficiently to prevent such interference, the problem was obviated by running the several units synchronously. Where other requirements dictated a different operating frequency, synchronization was maintained to avoid beats between them by operating at harmonically related frequencies.

The modification to the units involved an input and an output cable connection to the back plane. The input connection was plugged into the crystal socket; the oscillator transistor then acted as an amplifier, taking the signal from the unit on its left and passing a portion of the output to the next unit on the right.

Thus with a simple change in plug, each unit could be used either in a group or alone by unplugging the cable from the input connector to the crystal socket and plugging in the crystal again.

Unit 104 was additionally fitted with a divide-by-two circuit and LC filter between the input and crystal socket. This system drove the output at half the frequency of the unit in the slot immediately to the left of it. With this scheme it is possible to run one, two, or three units at 1 MHz, and

the remaining three, two, or one units at 0.5 MHz, as shown in Table 1. The operating frequencies are based on a 1-MHz quartz crystal in Unit 101. If a different frequency is used, the filter circuit in Unit 104 will need retuning.

4. CALIBRATION

The output frequency or output voltage of the analysis is primarily a function of the weighted average frequency of the broadband signal being analyzed. It is explained in Sec. 3.4. The system generates a tone with frequency 100 times the weighted mean of the spectrum. This tone controls a filter yielding a signal with half the energy of the original signal.

4.1 ELECTRICAL

Electrical calibration usually is done in two steps:

1. A low-pass filtered white noise electrical signal is injected into the analyzer system and the output frequency f_o is plotted against the cutoff frequency f_i of the signal, and a regression line is determined; the voltage output can be calibrated at the same time by reading the output voltage V_o--but it is easier to read V_o with a pure tone injection and obtain the $V_o - f_o$ function with the steadier pure tone signal, and

2. The $f_o - f_i$ transfer function is combined with the $V_o - f_o$ function to obtain the $V_o - f_i$ function.

It is a good deal easier to average a frequency than a voltage, because to better average the frequency it is necessary only to count longer, whereas the reading of a voltmeter (which is unsteady) is not straightforward, and different techniques yield slightly different results.

4.2 FLOW LOOP CALIBRATION

A flow loop was built with a weigh tank to determine the output of the flowmeter with the mass flowrate of fluid flowing (see Figs. 18 and 19). The loop consists of a 4-m (12-ft) vertical 102-mm (4-in.) ID pipe, a 1-m (3-ft) horizontal section, and a short vertical down section followed by a 2-m (6-ft) test section (mostly 2-in. pipe). From there the flow comes back up to a 1-m level to a tee followed by a pair of interconnected ball valves A and B, arranged so that one opens when the other closes. In one position the flow is taken back to the reservoir tank, mounted directly over the pump, which discharges the fluid into the 4-in pipe. The common handle of the ball valves, when thrown in the opposite direction, stops the fluid recirculation and

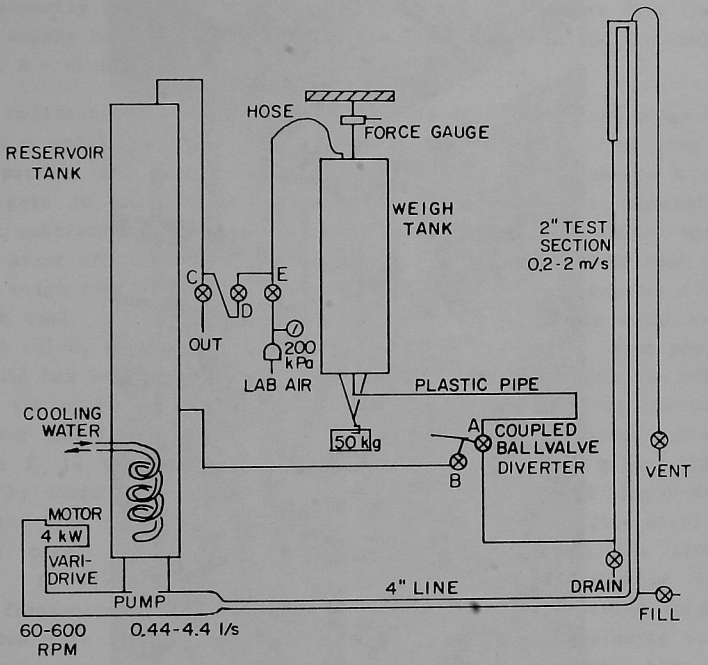

Fig. 18. Schematic of Flow Loop.

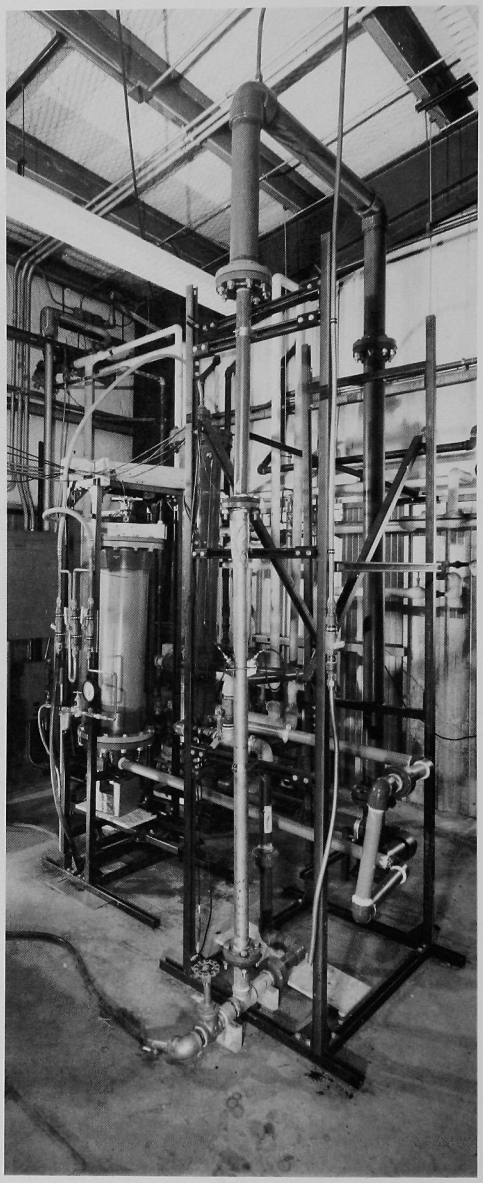

Fig. 19. Loop for Flowmeter Calibration.

diverts the fluid into the weigh tank. The fluid enters the weigh tank from the center of the tank base via a 2-m-long horizontal plastic 50 mm (2-in.) pipe. The top of the weigh tank connects via flexible rubber hose and three control valves to the top of the reservoir tank, the atmosphere, or the laboratory pressure supply. During normal operation the fluid is first circulated steadily at about ~150 kPa (22 psi) static pressure from the laboratory air supply in the gas space above the fluid level in the two tanks (valve A - open, B - closed, C - closed, D - open, E - open).

For calibration at that setting, fluid is diverted to the weigh tank (A - closed, B - open). As the mass of fluid increases, the output from the load cell supporting the tank falls and, at a preset point, starts a clock and opens a gate to start counting the pulses from the pulse repetition rate generator controlling the variable filter of the Doppler flowmeter being calibrated. After the clock and the counter have started, a 50-kg mass suspended from the weigh tank is gently raised so that it no longer touches any part of the weigh tank. The output of the load cell supporting the weigh tank jumps to a high value, decreasing slowly as more fluid is added. When precisely 50 kg of fluid has been added, the load cell output again reaches the trip level, stopping the clock and the repetition rate counter. If N is the reading of the counter and T is the reading of the clock, then the output pulse repetition rate f_o is N/T Hz at a mass flowrate of 50/T kg/s. Volume flowrate is computed by dividing mass flowrate by specific gravity, and linear velocity u is computed from this by dividing volume flowrate $\dot{Q}$ by the pipe sectional area S. The total count N remains reasonably constant as the flowrate is changed. It will be different for different wedge angles or ultrasonic carrier frequencies. To obtain the best value, the measured output pulse repetititon rate f_o is plotted as a function of linear velocity u, and the linear regression coefficient is obtained for this pair of variables.

After the clock and counter have accumulated the run data, the operator immediately resets the diverter valve pair back to circulation. Then the data, time duration, and number of pulses are recorded. The weigh tank is isolated from the reservoir tank, which is allowed to return to room pressure (valve D - closed, C - open). With the diverter valves (A, B) placed halfway between the diversion and recirculation position, both are half open and the laboratory air supply will push the fluid out of the weigh tank into the system. A digital voltmeter on the output of the force gauge is used by the operator to place the diversion valves (A and B) back to recirculation before the weigh tank is quite empty. The reservoir vent C is closed again and valve D connecting the air return of the weigh tank with the reservoir tank is opened to permit repeating of the cycle.

4.3 DATA

A typical set of calibration curves is shown in Figs. 20-24. The relation of the output voltage V_o to the repetition rate f_o of the filter control signal is plotted for several range settings in Fig. 20. Note that variable resistors P1 or P2 can be set to any value between the extremes shown by 1 and 2. Capacitor switches 3, 4, 5, and 6 change the range in steps.

This particular unit (Serial 111) is installed at the SRC-I pilot plant, with the switch setting and P1 adjusted as shown by the heavy line. For the other lines shown, P1 was adjusted to the extreme position opposite that of P2. The range of repetition rates for 10 V output for each capacitor position, seen at the right ordinate, is summarized in Table 2. These data were obtained by injecting a pure tone into the calibrate terminal. Individual points are not shown, the departure from a straight line is not appreciable on this scale.

The output repetition rate f_o is plotted as a function of the cutoff frequency f_i of filtered white noise in Figs. 21 and 22. (For these graphs, the cutoff filter was a Rockland low-pass elliptical filter with 85 dB per octave cutoff.) Note that the dial setting on the Rockland filter is the frequency at which the filter first passes the bottom of the pass band ripple, and not the frequently used 3-dB down point. The 3-dB point was measured consistently 5% higher than the cutoff frequency indicated on the dial. The numbers at the abscissa of Figs. 21 and 22 correspond to the numbers on the Rockland filter dial. Figure 22 is an expansion of the lower portion of Fig. 21. This portion is of greatest interest in situations encountered in coal liquefaction slurry flow. The full range was needed for the SLTF loop. It is immediately apparent that the range setting of the voltage output has only a second-order effect on the f_i-f_o transfer function, but the effect needs to be known for precision calibration.

The electrical calibration was compared with direct measurement of flow as determined by direct weighing (see Fig. 23). The result of this measurement was combined with the output of Fig. 22, showing the relation of the output to the input bandwidth to yield a measure of the effective or equivalent bandwidth of the input spectrum (see Fig. 24). The transfer was done by linear interpolation, point by point. The slope of this line is now compared with the computed Doppler slope in the absence of any profile correction outlined in Sec. 3 to yield a measured profile correction term.

The substitution $f_i = 2f_d = 4f_t \frac{u \cos\theta}{c}$, $f_t = 5 \times 10^5$Hz, $\cos\theta = 0.5047$, $c_{lucite} = 273000$ cm/s yields

$$f_i/u = 4f_t \cos\theta/c = 3.70 \ . \qquad (19)$$

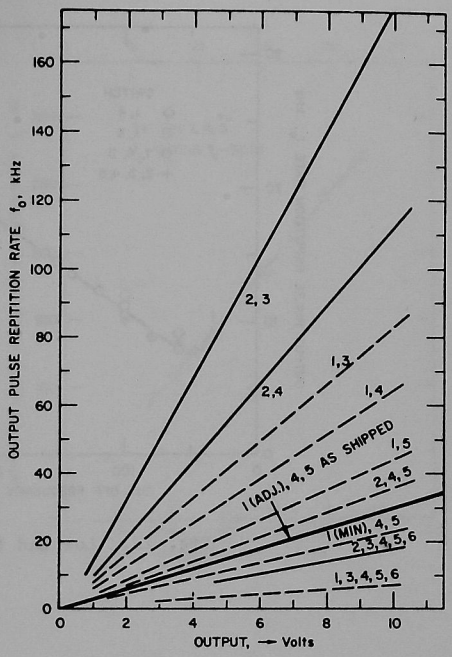

Fig. 20

Relation Between Output Voltage and Output Pulse Repetition Rate for Different Range Settings. [One or two using capacitors 3, 4] 5, and 6, or any combination. Rheostats 1 or 2 in their extreme positions, except that 1 (adj.) 4, 5 is the adjustment currently used at SRC-I.

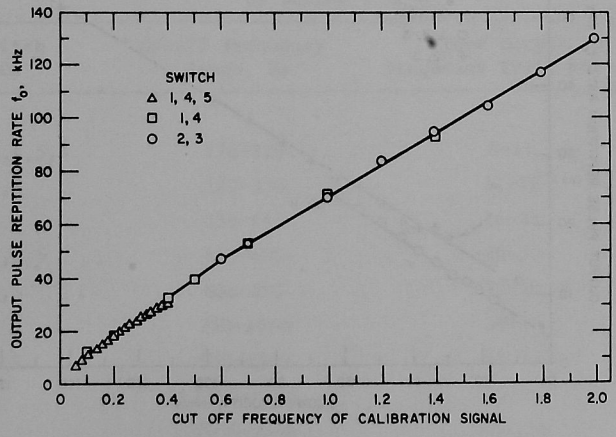

Fig. 21. Electrical Calibration Using White Noise with Sharp High-frequency Cutoff.

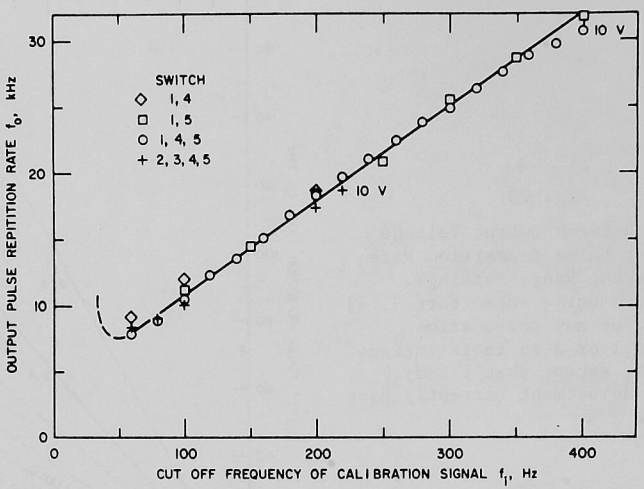

Fig. 22. Low End Expansion of Fig. 21.

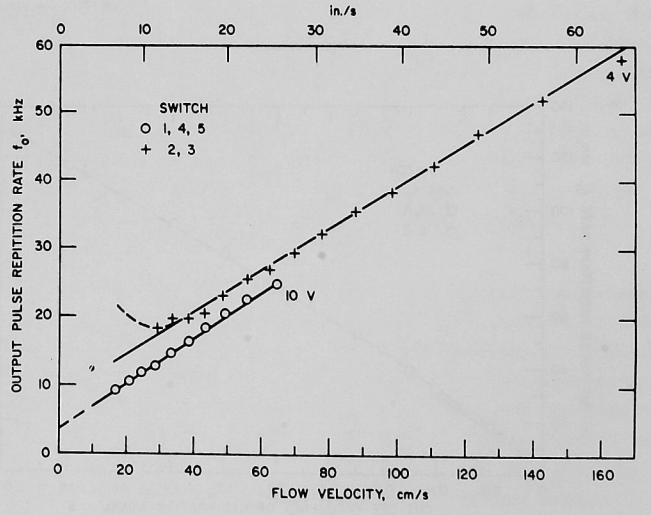

Fig. 23. Repetition Rate, Measured for Different Mean Flow Velocities.

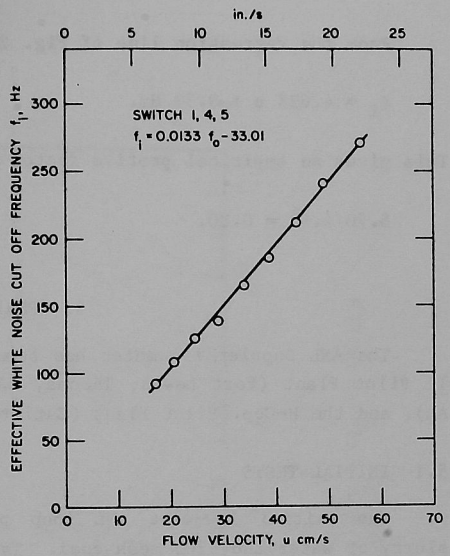

Fig. 24

Equivalent White Noise Band Cutoff for Doppler Spectra as a Function of Mean Flow Velocity.

Table 2. Range Adjustment for 10-V Output Using Potentiometer P1 or P2 as Selected by Switch 1 or 2

Switch On	Cutoff Frequency Range, Hz	Clock Output Frequency TP11, kHz
3,4,5,6	170-220	8-11
5,6	220-330	11-17
6	330-440	16-22
3,4,5	400-600	20-30
4,5	600-800	30-40
5	750-1000	38-50
3,4	900-1500	45-75
4	1300-1800	65-90
3	1600-2400	80-120

From the regression line of Fig. 24, we obtain

$$f_i = 4.62\ell\, u + 9.59 \text{ Hz}. \quad (20)$$

This gives an empirical profile factor of

$$3.70/4.62 = 0.80. \quad (21)$$

5. PERFORMANCE

The ANL Doppler flowmeter has been used on different ANL loops, the SRC-II Pilot Plant (Fort Lewis, Tacoma, WA), the SRC I Pilot Plant (Wilsonville, AL), and the H-Coal Pilot Plant (Catlettsburg, KY).

5.1 INITIAL TESTS

The initial low-cost ANL loop performed very satisfactorily[9] using a slurry of water and -200 mesh coal. Typical spectra are shown in Fig. 7. The electronic analyzer interpreting the Doppler signal in the initial flowmeter was a simple counter circuit that treated the Doppler signal as though it were a pure tone, counting the cycles. A few refinements were added to the original simple frequency counter. A fixed-threshold comparator with some hysteresis was used to prevent low-level high-frequency noise from adversely affecting the counter. A good-quality low-pass filter required to eliminate the noise above the highest Doppler frequency also is effective in keeping the count correct. The final calibration using a weigh tank is shown in Fig. 25.

Subsequently, the loop was modified to the configuration described in Sec. 3 to eliminate cavitation bubbles, which were demonstrated conclusively to have existed in the open loop as originally configured. The discovery was accidental when the loop was used to test immersed transducers. It was found that sound propagation of 5 MHz for a 30-cm (1-ft) distance disappeared (i.e., there was more than 60 dB additional attenuation) when fluid flowed in the pipe. Sound transmission returned within a few minutes of flow cessation. Sound propagation also could be restored by pressurizing the loop to about 30 kPa (5 psi). Pressure release stopped propagation. Although the bubbles were not visible because they were too small and the fluid was too opaque, the evidence is clear. Modifying the loop to eliminate the cavitation bubbles was considered important to test flowmeters for more realistic situations. The presence of the small cavitation bubbles greatly enhances the strength of the Doppler signal. The calibration figure (Fig. 25) tends to indicate that the total volume of cavitation bubbles was sufficiently low that the mean density

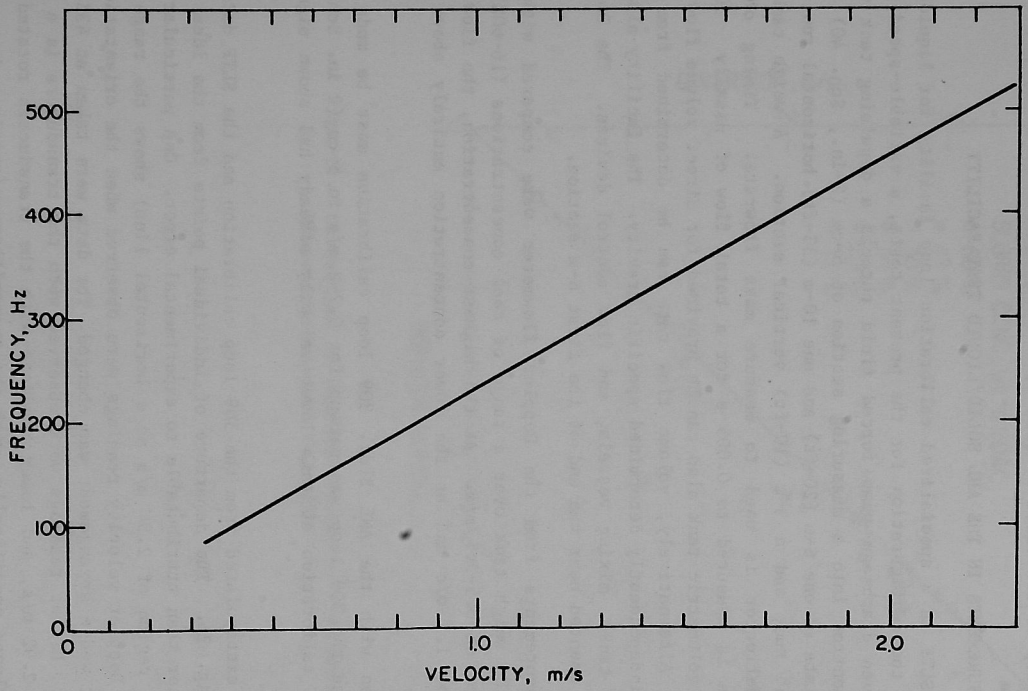

Fig. 25. Doppler Flowmeter Calibration with a Low Viscosity Water/Coal Slurry (turbulent flow).

of the fluid was not changed significantly by the presence of the minute void fraction. Additional evidence for this estimate might be worth gathering if the opportunity should arise. Turbulent flow measurement was completed before the existence of cavitation throughout the loop was recognized. Operation of the modified loop is described in Sec. 4.

5.2 FLOW MEASUREMENTS IN THE ANL SOLID/LIQUID TEST FACILITY

The ANL SLTF is a specialized calibration loop facility for liquids and slurries. In the configuration for the present tests, a variable-speed pneumatically driven diaphragm pump forced fluid through a depulsing tank via a bypass flow control into a measuring section of 5-cm (2-in., Sch. 40) pipe. The pipe consists of one 6-m (20-ft) and one 10-m (33-ft) horizontal run, a 2-m (6-ft) 45° run, and a 3-m (10-ft) vertical section. A weigh tank and fast-action deflector is used to measure mass flowrate. Timing of the diverter valve is measured to 0.005 s for a total flow of usually ~50 kg. Transfer to a volumetric tank also can be provided for direct volume flow rate measurement. Alternatively, volume flow rate can be determined from mass flowrate and independently determined specific gravity. The facility also includes holdup tanks, mixing vessels, and flow control devices. The Doppler flowmeter was mounted near the end of the first 6-m section.

Flow measurements from the Doppler flowmeter were compared with the readings of the weigh tank over a range of coal concentrations (16-60%) for flow velocities of 0.5-3.5 m/s. At the highest concentration, the flow rate was kept below 1.3 m/s and at the lower concentration entirely above this minimum value.

Comparison with the ANL Bldg. 309 loop calibration must be made with caution because the 309 loop was set up for 0.2-2 m/s in 5-cm (2 in. Sch. 40) pipe, and the calibration at this lower velocity already had shown signs of nonlinearity.

Readings extrapolated from the 309 loop calibration and the SLTF data are compared in Fig. 26. The departure of individual points from the ideal line shown is greater than attributable to experimental error. One particular area (shown in the region of 2.54 m/s as a horizontal line) shows the range over which several Doppler velocity readings were observed when the orientation of the transducer wedge arrangement was changed. The data were taken at 43% coal concentration. Higher readings were observed with the transducers in a horizontal plane, 2.92 m/s, and lower readings with the transducers rotated into the vertical plane; specifically, with the transmitter-up/receiver-down orientation, the effective reading was 2.06 m/s, and with the opposite connection (transmitter down), the reading was 1.93 m/s.

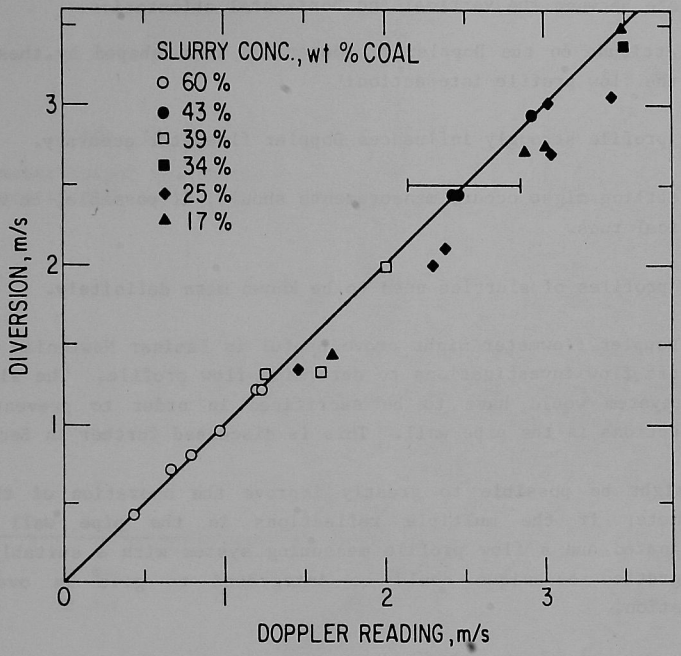

Fig. 26. Comparison of Doppler Flowmeter Velocity with SLTF Diversion Measured Velocity.

Spectra obtained during these runs (Fig. 13) showed an intense low-frequency contribution that was much more pronounced when the transducers were oriented in the vertical plane than when they were in a horizontal plane. With the transducers oriented at 45°, the spectra and readings (2.63 m/s) were intermediate between the vertical and horizontal orientation.

Our attitude on the Doppler flowmeter has been shaped by these observations on the flow profile interaction:

Flow profile strongly influences Doppler flowmeter accuracy.

If settling might occur, measurements should, if possible, be confined to vertical runs.

Flow profiles of slurries need to be known more definitely.

The Doppler flowmeter might prove useful in laminar Newtonian or pseudo-plastic flow investigations to determine flow profile. The simplicty of the system would have to be sacrificed in order to prevent multiple reflections in the pipe wall. This is discussed further in Sec. 7.

It might be possible to greatly improve the operation of the Doppler flowmeter if the multiple reflections in the pipe wall could be eliminated and a flow profile measuring system with a suitably weighted integration technique could be integrated to give an overall flow summation.

5.3 FLOWMETERS ON SRC-II

The intermittent operation of the early model ANL flowmeter led to the development of the instrument described in Sec. 3. The flowmeter installed was a rough model of the final version, the plant being dismantled before construction of the final instrument was completed. The final instrument, described in Sec. 2 and Appendix A, was originally designed with specifications for SRC-II operation. The final system was installed on the H-coal pilot plant.

On the SRC-II plant, two positions were monitored. The first was the coal feed line described in some detail in Sec. 3. The flowmeter installed on this line generated many of the lessons outlined in Sec. 3. The rough model of the ANL flowmeter was connected to the SRC-II data acquisition system. The data output was manually plotted from the acquired data, and is reproduced here as Figs. 27 and 28. The same electronic system also was connected to transducers mounted on the recycle line. Particulates in this line were

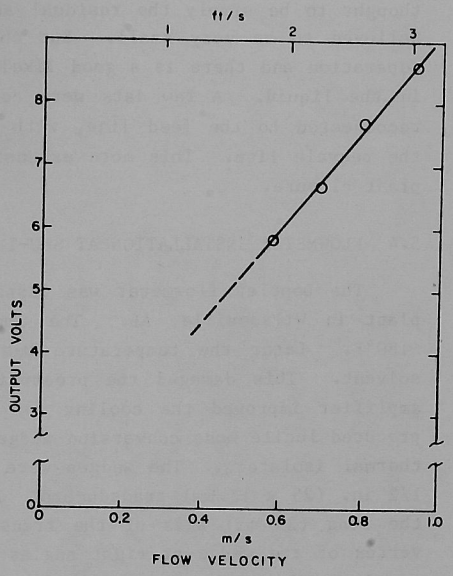

Fig. 27

Flowmeter Output vs. Material Balance at SRC-II.

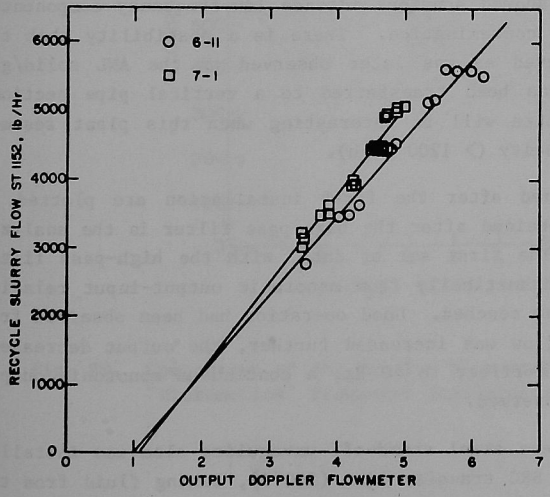

Fig. 28

Flowmeter Output on the Recycle Line of SRC-II Using Close Coupled Transducers.

thought to be simply the residual ash particles of undissolved coal and were believed to be very small. But this line follows immediately a liquid/gas separation and there is a good likelihood of microbubbles remaining entrained in the liquid. A few data were collected before the electronic system was reconnected to the feed line, with later scheduling of data collection from the recycle line. This more extensive data collection was eliminated by the plant closure.

5.4 FLOWMETER INSTALLATION AT SRC-I

The Doppler flowmeter was installed on the coal feed line at the SRC-I plant in Wilsonville, AL. The temperature of this line was estimated at ~180°F. Later the temperature was raised occasionally to 350°F using hot solvent. This damaged the preamplifier and the wedges. Relocation of the amplifier improved the cooling for it. In this installation, commercially procured lucite mode conversion wedges were used directly without any standoff thermal isolators. The wedges were specially made for use with the 1 in. x 1/2 in. (25 x 12 mm) transducers. A departure from conventional design made the long (25 mm) axis of the transducer parallel to the pipe axis and the vertex of the wedge at right angles to it. The lucite wedges were cast in a sound-absorbing plastic to reduce spurious reverberations in the wedge. The wedge and transducer and the wedge and pipe were coupled with petroleum jelly.

Spectra from this line showed spurious intense low-frequency components. There appeared to be no gas contamination. There is a possibility that the same type of settling occurred as was later observed on the ANL solid/gas facility. This flowmeter has been transferred to a vertical pipe section. Reevaluation of Doppler spectra will be interesting when this plant resumes operation at a high flow velocity (> 1200 lb/h).

The initial data obtained after the first installation are plotted in Fig. 29. These data were obtained after the high-pass filter in the analyzer section was set to 40 Hz. The first set of data, with the high-pass filter set to 25 Hz, had departed dramatically from monotonic output-input relation when the maximum flow rate was reached. Good operation had been observed from 500-1000 lb/hr flow. When flow was increased further, the output decreased. After adjusting the high-pass filter to 40 Hz, a continuous monotonic output voltage with flow rate was observed.

A flowmeter with stainless steel stand-off waveguides also was installed later (Oct. 9, 1982) on the SRC transfer line (550°F), taking fluid from the dissolver to the de-ashing unit of the plant. Operation was better at 1 MHz than at 500 kHz. By this time we had learned the need to synchronize the oscillators of the two units, as described in Sec. 3. The high-temperature unit was operated at 1 MHz and the low-temperature unit for the feedline

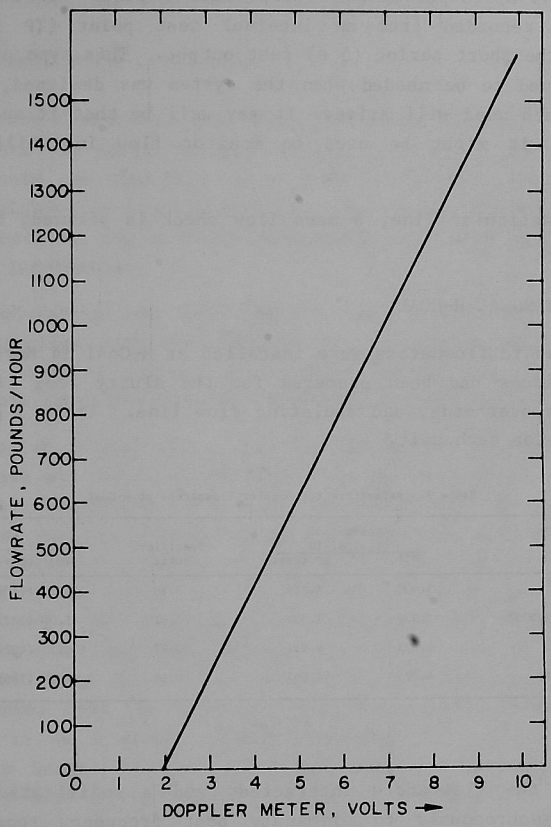

Fig. 29. Comparison of the Doppler Flowmeter at SRC-I against a "Micromotion" Flowmeter Standardized with Mass Flow Calibration.

operated at exactly half that frequency.

The spectrum from this flowmeter had the desirable sharp cutoff shape. Of particular interest was that during a very brief period, this line was operated by a 45-cycle-per-minute reciprocating pump. Individual slugs of fluid could be recorded from an internal test point (TP 10) before the integration of the short period (5 s) fast output. This type of fast response was not envisioned to be needed when the system was designed, and it is not clear whether such need will arise. It may well be that if such a capability were available, it might be used to monitor flow instabilities or other faults.

For this particular line, a mass flow check is planned, but has not yet been implemented.

5.5 FLOW MEASURING AT H-COAL

Four ultrasonic flowmeters were installed at H-Coal in March 1982, during Run 9. Spoolpieces had been prepared for the slurry feed line, hydroclone feed, hydroclone overheads, and ebulating flow line. Table 3 gives the relevant parameters for each unit.

Table 3. Parameters for Doppler Flowmeters at H-Coal

Unit	Nominal ID of Pipe, in		Specific Gravity	Alarm Flow, TPPH* (cm/s)	Particle Size, μm
	70°F	OP.Temp.			
Slurry feed (FR256)	3.000	3.012	3.10	71.12 (177)	75
Hydroclone overhead (FIC275)	1.939	1.950	0.92	45.38 (323)	10-20†
Ebulating flow (FR230)	6.875	6.931	0.82	636.7 (402)	10-20†
Hydroclone feed (FIC266)	4.026	4.052	0.83	80.0 (146)	10-20†

*Thousand pounds per hour.
†Depends on coal used.

Initially, the flowmeters interacted, and a modification was made to operate them synchronously to eliminate beat frequency tones between the units. This method was easier than trying to improve interchannel isolation. The modifications were completed within a few weeks, and the installed units were retrofitted in June during Run 10. The output voltage of the Doppler flowmeters was sent to the plant data acquisition system and stored. At the end of Run 11, data were retrieved and plotted together with the stored reading of other flowmeters on the same lines.

The initial interferences between the separate units permitted valid data from only one unit (FR256) during Run 9. During Run 11 this particular line was not in use, so FR256 is reported for Runs 9 and 10. Data for line FIC266 are given for Runs 10 and 11. The spoolpiece for this particular line is

shown in Fig. 1. Two transducer arrangements were used:

A commercial transducer sold for nondestructive testing; it was coupled to the pipe via a mode conversion plastic wedge, and a heat isolating standoff waveguide brazed to the pipe, and

A high-temperature transducer.

High-temperature transducers generate shear waves directly, using a crystal of lithium niobate cut normal to the X-axis. A small inconel wedge couples the shear waves into the pipe wall at an angle of 27° with the pipe axis. During Run 10, the high-temperature transducers were used; during Run 11, the commercial transducers on the standoff waveguides were used with equal success to provide flow information.

On the ebulating pump line (FR230), data were gathered on Run 11. Data from the hydroclone overhead (FIC275) were discarded when it was determined that erratic behavior was due to a broken braze joint between the waveguide and pipe. This shows the need for improved quality control in this area.

The Doppler signal--that is, the difference between the transmitted ultrasonic wave and the received signal--is in the form of a noise-like signal combining many frequencies up to some maximum value. For turbulent flow, the Doppler signal contains mostly frequencies near the average value; intensity at lower and higher frequencies falls rapidly. In laminar flow, the distribution is broader; the intensity is fairly constant from zero to about twice the average frequency. We observed this typical flat spectrum on Line 256, indicating that on this line there was probably quite a bit of multiple scattering and the sound field was fairly uniform across the pipe. On other lines, spectra departed from the expected laminar or turbulent shape. In general, they tended to be a simple gradual decrease in intensity without a well-defined sharp break. In one instance, strong fluctuations in the spectrum were observed over a short period of just a few minutes. The Doppler meter will find some average value of the spectrum here, but so many factors influence the shape that it becomes difficult to separate velocity effects from others.

We know that in viscous fluids with extremely fine particles, scattering is poor and there is high loss due to viscous friction. As a result, the sound beam is much weaker near the center of the pipe than near the surface, and we see a dominance of scattering by the slower peripheral particles. At first it was hoped that by placing a transmitter and receiver on opposite sides of the pipe this could not happen; however, as illustrated in Fig. 30, the sound beam reflects many times in the pipe wall, and after several reflec-

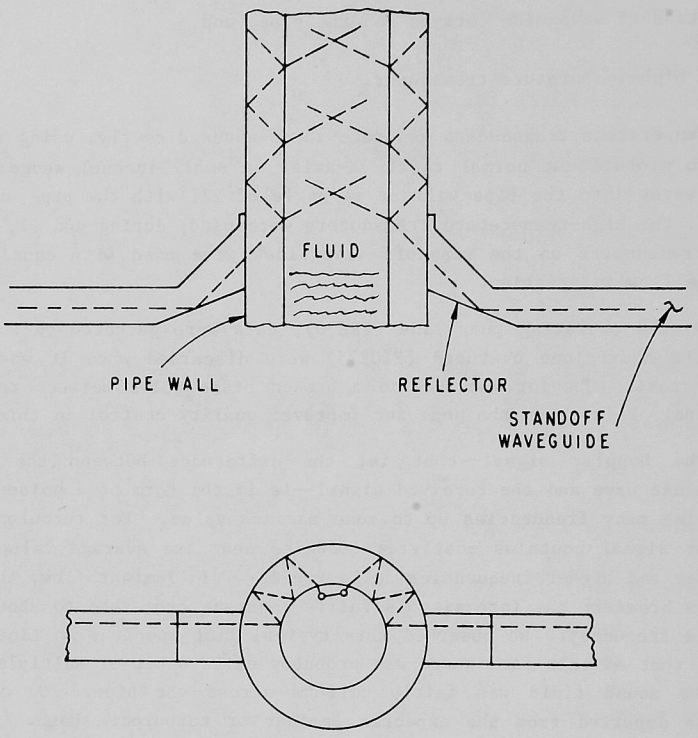

Fig. 30. Schematic of Pipe at H-Coal. The high reflection coefficient at the wall surface allows sound energy to be transmitted dominantly via scatterers close to the wall.

tions, spreads around the pipe. This can be seen in the lower part of Fig. 30 in the plan view of the pipe. Thus particles near the wall will be measured with only very slightly diminished amplitude, whereas the scattering from the central region is strongly attenuated.

The Doppler meter was operated experimentally with different frequencies in the range 0.3-5 MHz. Both attenuation and scattering increase with frequency and particle size. For very small particles, adequate scattering requires a high frequency, which, in turn, is subject to greater attenuation. Frequency was varied from 0.3 to 5 MHz using a very stable synthesizer. Much of this work was done on one line, using the broadband high-temperature transducers. On other lines, special broadband transducers were used from 0.3 to 2.5 MHz. Standard resonant transducers also were used over an appreciable range near resonance, using separate commercial units tuned to 0.5, 1, 2.25, and 5 MHz.

Even though the desirable shape of the spectrum could not be obtained on the ebulating pump flow (FR230) nor the hydroclone feed (FIC266), the Doppler flowmeter responded to velocity fluctuations. Daily averages of flow rate in thousand pounds per hour are plotted in Figs. 31-35, which were produced directly by the computer at H-Coal with only the abscissa altered for greater reader convenience. Each graph shows daily averages of both the Doppler meter and the installed meter.

One design modification of the Doppler meter is still needed. As shown in Fig. 31, intermittent loss of flow April 12 and 13 caused the Doppler meter to amplify residual noise, which is broadband, and it thus indicated full scale. The same situation arose after completion of Run 10 after July 22. A sudden change in the calibration factor the day after adjustment on June 18 has not been explained. In Run 11, slurry was fed through a different unmonitored line and no data were collected.

In view of the poor spectrum obtained, surprisingly good correlations between the installed orifice meter and the Doppler meter were obtained for the hydroclone inlet and ebulating pump. The sudden change in the sensitivity on August 23 is puzzling. The two meters were realigned on Sept. 14. On Oct. 4 the orifice meter apparently failed; when it was brought back online Oct. 8, the difference between the two meters is as likely due to the orifice meter as to the Doppler meter.

After the Sept. 14 realignment, the ebulating pump flowmeter remained reasonably good for the rest of the run. The orifice meter failed early in November and plant operators relied on the Doppler meter for the last few days of the run.

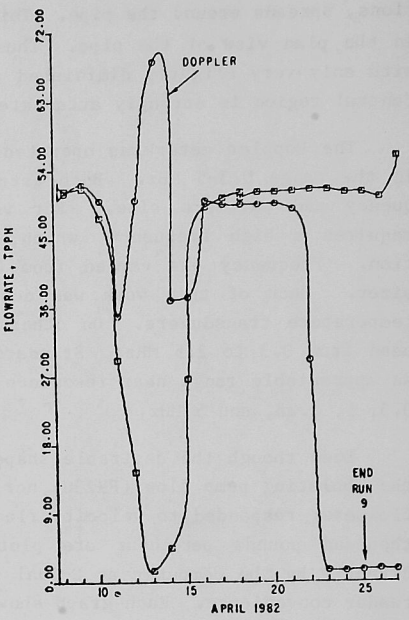

Fig. 31

Comparison of Doppler Flowmeter on Slurry Feed Line with Installed Meter (Run 9). Slurry feed line loss of flow April 12 and 13 caused the Doppler meter to go to full scale.

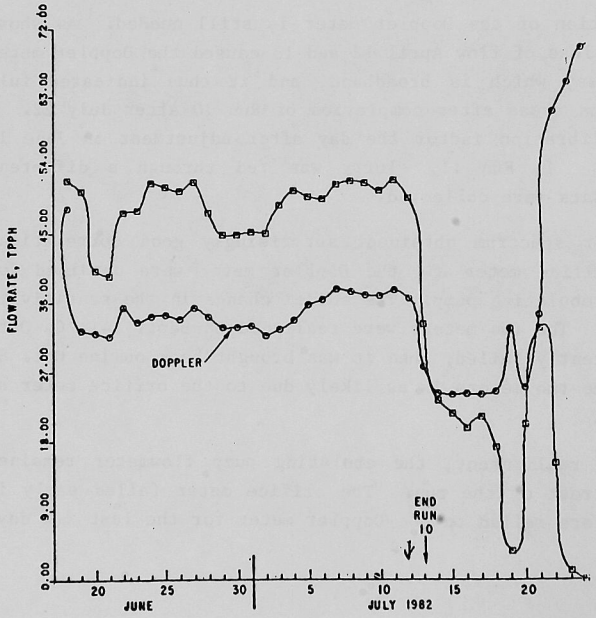

Fig. 32

Comparison of Doppler Flowmeter on Slurry Feed Line with Reference Plant Meter (Run 10).

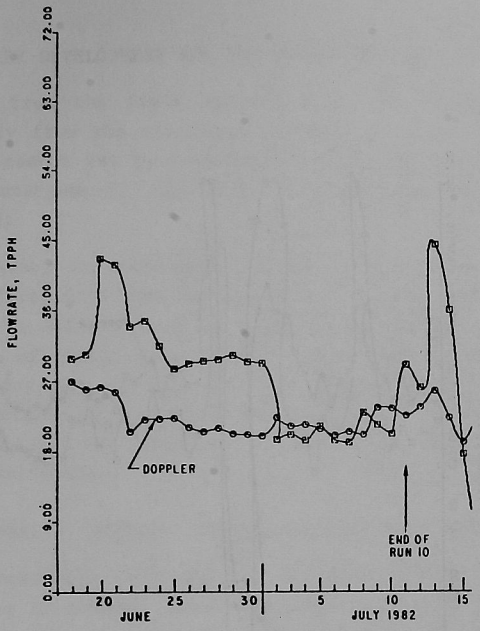

Fig. 33. Comparison of Doppler Flowmeter at Hydroclone Inlet with Reference Plant Meter, 4-in. Pipe, Run 10.

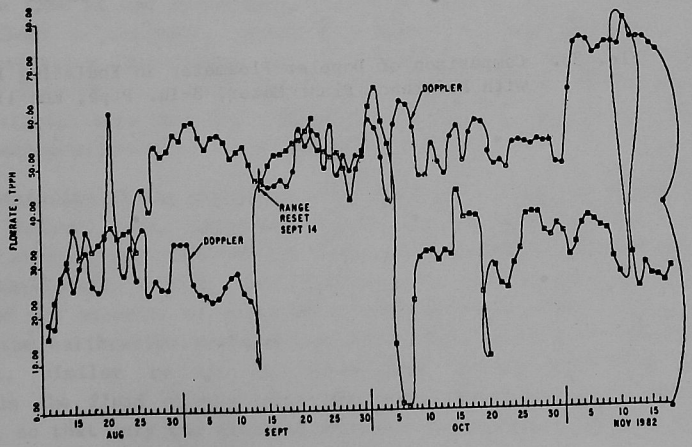

Fig. 34. Comparison of Doppler Flowmeter at Hydroclone Inlet with Reference Plant Meter, 4-in. Pipe, Run 11.

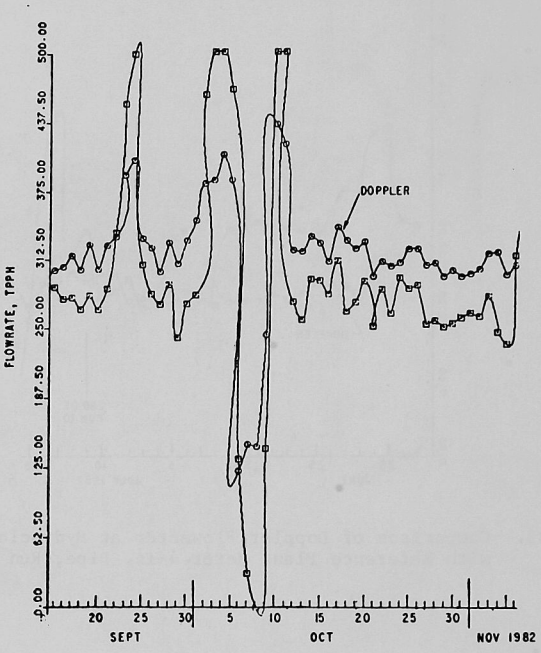

Fig. 35. Comparison of Doppler Flowmeter in Ebulating Flow with Reference Plant Meter, 8-in. Pipe, Run 11.

6. FURTHER DEVELOPMENT FOR THE ULTRASONIC DOPPLER FLOWMETER

It is clear from the field studies that the conditions in the field differ sufficiently from the simulated conditions in the laboratory that the Doppler flowmeter cannot yet be considered a fully developed universal instrument, applicable everywhere. Specifications and application limitations are noted in Section 2.

Improved accuracy is obtainable if the flow profile is determined. To determine the profile, flow must be measured in a more restricted region. The Doppler flowmeter is eminently suitable for this, provided we give up the very attractive feature of clamping transducers on an existing pipe system. If the transducer is in intimate contact with the fluid, it is possible to interrogate different portions of the fluid by time gating. Additional measures of velocity distributions are possible by aiming beams along chordal planes instead of diametral planes.

6.1 IMPROVED ACCURACY: DOPPLER FLOW MEASUREMENT BY PROFILE ANALYSIS

With the transducers attached to the outside of a uniform pipe, very little can be done to measure specific small regions of the flow because the sound wave bounces back and forth inside the pipe wall, with only a small fraction (1-5%) depending on sound impedance of the fluid penetrating into the fluid at each impact. After a few reflections, the sound wave is extended over a large part of the pipe wall (Fig. 30). Then the scattered energy from particles close to the wall, after many reflections inside the wall, arrives at the same time as the sound wave, which penetrated to a deeper layer with few reflections in the wall. Thus, time-gating has proved very ineffective with nonpenetrating transducers, but is expected to be quite effective with transducers immersed in the fluid or in a coupling fluid and separated from the abrasive/corrosive flowing slurry by a thin, acoustically transparent window. Another alternative is discussed in Sec. 6.2.

Implementation of the system is shown in Figs. 36 and 37. Figure 36 is a conceptual layout, using immersed high-temperature transducers. They are shown here with a wedge between the transducer element and the fluid. With immersed transducers, a flat face (flat on both sides) would work; however, knowledge of the velocity of sound would then be required to compute the flow rate, and the calibration would change with sound velocity. With the wedge arrangement, similar to the non-penetrating transducers, the angle of incidence in the fluid changes with the sound velocity and the two effects compensate, so that only the velocity of sound in the wedge must be known.

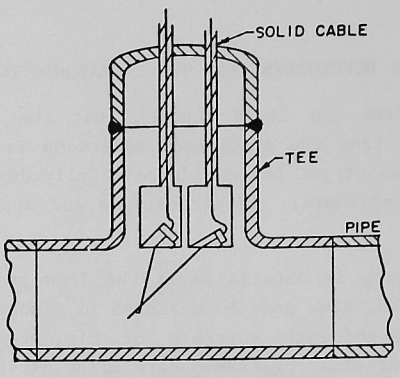

Fig. 36. Immersed Transducer in a Tee Connector. Tone burst will be transmitted to select a specific region of the pipe.

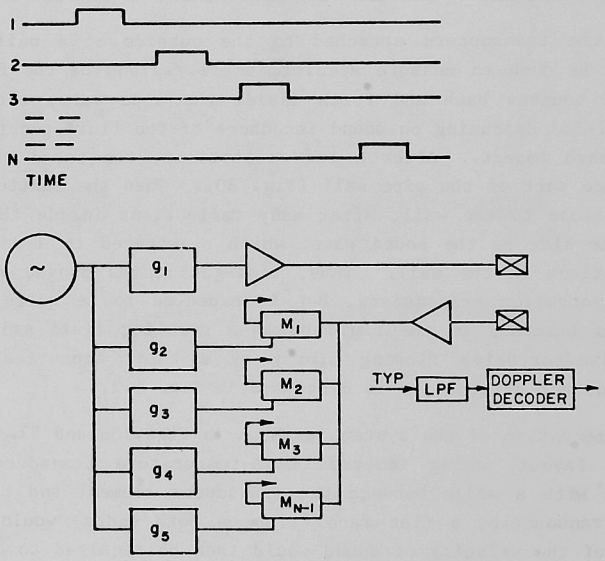

Fig. 37. Time-gating System for Flow Profile Studies and Precision Doppler Flow Measurement.

Transducers are shown deployed in two locations to sample different planes of the pipe. The specific region along the length of the beam can be resolved by time gating. Algorithims must be developed to properly weight the separate regions of flow.

The electronic system would, of course, also be more complex (Fig. 37). One gate provides a short tone burst to the transmitting transducer and another supplies a tone burst to each receiving mixer, which then acts both as mixer and gate for the ultrasonic carrier. This type of circuit, with a single-channel variable gate receiver, was tried in the early experiments at SCR-II. As a circuit, it worked very well, but nothing was gained by tone burst operation. The reason for this was the multiple reflections of the ultrasonic beam in the pipe wall; the reflections prevented pinpointing any one region within the pipe, because the sum of the different delays in the pipe wall and in the fluid prevents differentiation of the signals from different parts of the fluid.

Time gating techniques have been studied for medical applications for measuring blood flow. Nonintrusive flowmeters have seen extensive development there, but the multiple reflections in the steel pipe wall is a problem unique to industrial application.

6.2 IMPROVED DOPPLER FLOW MEASUREMENT BY PROFILE CONSTRAINT

As an alternative to the detailed measurement of the flow profile outlined in Sec. 6.1, it might be possible to make use of the fact that the ultimate profile takes a long distance to develop. Immediately following a constriction, the flow profile is fairly uniform except for a negligibly small region adjacent to the wall. Thus the profile of the flow velocity resembles the turbulent profile more than the laminar profile usually found in slurries. The measurement of flow in this region could be implemented using an immersed transducer combined with the time gating described in Sec. 6.1.1. Alternatively, it might be worth exploring the possibility of using external transducers and effectively decoupling the sound beam from the remaining piping system with spacers isolating the pipe wall from the ring forming the constriction, as shown in Fig. 38. Then tone bursts and time gating would still be meaningful with the elimination of the multiple reflected beam along the pipe wall. The high-temperature transducer and waveguide shown in Fig. 38 are illustrated as alternative designs and are not recommended for simultaneous use.

The optimum area reduction would depend on the rheological property of the fluid. Preliminary analysis indicates that for a Newtonian fluid, a flat profile would be obtained for a 30% diameter reduction; then the average velocity would be equal to the peak velocity ahead of the constriction. For

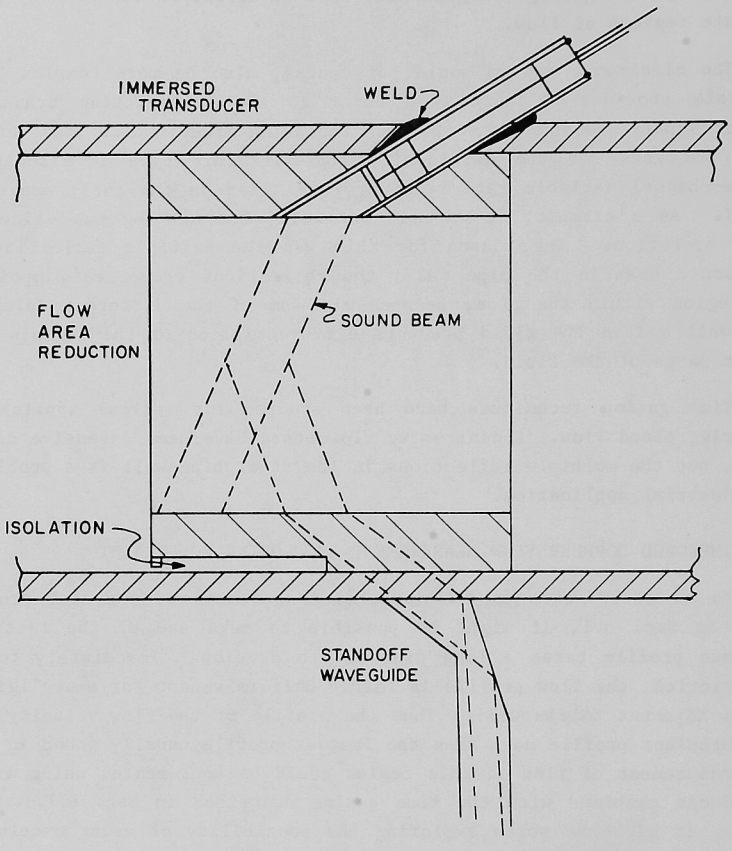

Fig. 38. Flowmeter Using Flow Profile Control at a Constriction. Isolation of the sound from extensive pipe wall regions may be effected by immersion (upper system) or suitable slots (lower system).

pseudoplastic fluids, this same area reduction would exceed minimum requirements for uniform flow immediately behind the constriction. Only with dilatant fluids, which increase shear stress with strain rate, would one need greater area reduction to assure uniform flow in the constriction. Our experience shows that slurries tend to be pseudoplastic and not dilatant.

The merits of the designs in Secs. 6.1 and 6.2 are that

Detailed study of flow is possible; the design in Sec. 6.1 yields useful information on rheological properties of the fluid and permits predictions of performance of the simpler types of flowmeter, and

The scheme described in Sec. 6.2 is simple, and can be combined with a time-gating probe and multiple transducers for chordal paths in addition to the diametral paths to permit detailed fluid flow studies and yield information needed for the calibration of an ultimate simpler flowmeter.

Pressure drop considerations produced by a short constriction are less significant in laminar flow than in turbulent flow. However, where this might be undesirable, a suitable length of oversize pipe could be incorporated into the flowmeter. The concepts developed in this section were developed during the writing of the report and so experimental exploration is beyond the scope of coverage.

6.3 RECOMMENDED STUDIES FOR SLURRY FLOW MEASUREMENT

The field tests of the Doppler flowmeter combined with the loop tests at ANL show a need for definitive answers to questions relating to flow with the particular devices tested. The answers needed relate to the following:

1. Acoustic attenuation as a function of sonic frequency, liquid viscosity, particle size, and concentration.

2. Flow profile in vertical pipes and the length after a disturbance (valve, tee, or elbow) before a predictable profile is achieved. For Newtonian fluids this information is known. For the pseudoplastic or thixotropic material research is needed.

3. Flow profile in horizontal pipes with a measurement of settling.

4. Design of a special acoustic Doppler flowmeter with window transducers so that with time gating, flow profile can be studied. (Single or dual transducer models might be suitable. A liquid column standoff or an immersed solid wave guide might be better. In

any event, to get such a system to work we must reduce the energy coupled to the wall.)

5. Possible simultaneous measurement of attenuation. It would be necessary to have another transducer pair facing normally on the pipe and measure the through transmission. This measurement of attenuation would then be used to correct the flow measurement for attenuation effects.

6. Improvement of the means of attaching the transducer standoff assembly. For applications to 250° C (500° F), plastic wedges and epoxy cements can be found. The brazing technique used on this project worked except for one failure. It is fairly expensive and difficult to apply in the field. Other fastening methods (e.g. welding, clamping, etc.) need to be checked out.

7. Less expensive methods of transducer assembly. The method of clamping high temperature transducers to the pipe has proved quite successful. The present method works quite well, and, in a somewhat similar transducer assembly on a sodium loop at EBR-II has lasted five years without significant deterioration.

7. DISCUSSION AND CONCLUSIONS

7.1 DISCUSSION

The Doppler flowmeter can be used to measure the flow of slurries provided that particles are above some minimum diameter. This minimum diameter has been shown to be less than 70 μm (0.003 in.) and is likely to be 30-50 μm. Tests with 20-μm particles in a viscous fluid resulted in a flow indicator with an output varying with flow but strongly influenced by other parameters. In extremely dilute slurry, in which there are only a few particles, it is possible to increase the operating frequency to so high a value that appreciable scattering is still obtained. However, with high-density slurries, there is a sharp cutoff between 20 and 70 μm.

A useful spectrum and good operation of the ANL Doppler flowmeter was obtained in slurry lines with fine particulates--the recycle line at SRC-II and the corresponding line at SRC-I coming straight from the liquid-gas separator after the first dissolving and heating of the coal. We suspect the presence of microbubbles in this effluent.

7.1.1 Observations

Two approaches to the problem of metering hot fluids were examined:

Standoff waveguides and

High-temperature transducers.

The standoff waveguides permit the use of conventional transducers normally supplied in the nondestructive testing market. This permits easy replacement in case of failure; long life can be expected with confidence. The couplant used between the transducer and wedge and the wedge and waveguide was a thin layer of petroleum jelly. For permanent installations, a longer-lasting couplant might be desirable. Cement, e.g., epoxies, often are used, but they have the disadvantage of making replacement more difficult. A suitable compromise might be a low-melting-point rosin that could be fused to the wedge and remelted to permit removal for replacement.

Attachment of the waveguide to the pipe by brazing proved less convenient than expected. For the larger pipes, there were difficulties in the field in applying sufficient heat to the pipe to make a good bond. The waveguides tested were all attached at the ANL shop to short pipe sections that were installed subsequently with flanges or by welding these spoolpieces in place. Even with this technique, one of the 14 brazed joints failed. More sophisticated inspection of brazed joints is needed and alternative techniques (e.g., welding) need to be investigated.

Use of high-temperature transducers clamped to the pipe was successful. Application of this technique had been demonstrated on a sodium flowmeter over a four-year period at temperatures of 540-870°F. The method is expensive, requiring the preparation of an optically flat surface over an area of 1.5 x 2.5 cm (3/4 x 1 in.)--a substantial task. Preparation at the ANL shop took more than a day for each surface. Developing less costly methods is desirable, but not as immediately urgent as establishing the operating problems.

7.1.2 Desired System Modification

The Doppler flowmeter circuit would be improved by having some form of alarm and cutoff when flow velocity falls to a value such that the Doppler frequency falls below the high-pass filter frequency or when there is loss of signal due to some other cause.

Another operator convenience would be an output offset adjusted to compensate for the internal output offset so that the output could be read directly on a strip chart recorder. This feature is not important for automatic data acquisition systems because such offsets can easily be taken care of by the data acquisition computer. Such a system has been installed at SRC-I since the ANL Doppler flowmeter was hooked to the system, and it is not unreasonable to anticipate ubiquitous data acquisition systems. In that case, there would be no need to modify each instrument. Other modifications in system operation also are discussed in Appendix B. These should be considered if widespread installation of the Doppler flowmeter is contemplated.

7.1.3 Direct Frequency Counting

The original simple zero-crossing counter worked well for the turbulent flow condition, but failed for the laminar flow case with the additional low-frequency component contamination. A low-frequency cutoff filter and a servo-mechanism spectrum measuring system were devised to determine the critical characteristics of the flat spectrum produced by laminar flow. A few measurements toward the end of the project indicated that the simple zero-crossing counter might also work for laminar-flow spectra if the spurious low-frequency components were eliminated. In other words, the number of zero-crossings of a wave having a flat broadband spectrum seems to be proportional to the average of the high and low cutoffs. The theory behind this is not understood as is the theory of the servo-controlled system. However, if the zero-crossing counter system could be verified, it would lead to a simpler system. This would be particularly desirable if the complexity of the system were augmented by the profile analysis discussed in Sec. 6.1.

7.2 CONCLUSIONS

Flow can be measured using the Doppler shift of backscattered ultrasonic signals from particles suspended in a fluid. The ability to transmit signals through the wall of the pipe without any holes is very attractive and the overall electronic system can yield an output voltage or current or frequency proportional to the velocity of the slurry in the pipe with relatively simple equipment. Good operation is obtainable for a slurry flow containing particles larger than $\sim 50 \pm 20$ μm (300 mesh). For slurries with only small particulates (<20 μm), the Doppler flowmeter has given indications of flow, but the magnitude was not always predictable or consistent. Good readings were obtained in two instances where the very fine particulates may have been augmented by the presence of microbubbles.

ACKNOWLEDGMENTS

This report covers a part of the overall synthetic Fuel Program effort at Argonne National Laboratory, sponsored by the U.S. Department of Energy. Work direction from DOE was provided by T. Simpson and S. Lee. N. O'Fallon managed the program until February 1983; A. C. Raptis has taken on responsibility as program manager. Additional supervisory management was provided by G. S. Rosenberg and T. P. Mulcahey.

Construction of the preliminary test loop and electronic test equipment was carried out by I. Pollack. The loop was rebuilt in its present configuration by W. Lawrence, who also assisted with data collection at SRC I. S. S. Sheen assisted with data collection at H-coal. T. L. Bernovich laid out and constructed the electronic circuits, and assembled the high-temperature transducers. G. Dusatko and others in ANL Central Shops fabricated the stand-off waveguides and wedges.

REFERENCES

1. J. P. Bobis, S. H. Sheen, K. G. A. Porges, H. B. Karplus, M. M. Farahat, W. M. Farahat, W. E. Brewer, N. M. O'Fallon, and A. C. Raptis, "Preliminary Report on Development of Nonintrusive Flow Instrumentation at the ANL Solid-Liquid Test Facility," Argonne National Laboratory report ANL/FE-83-18 (1983).

2. K. Porges, S. Cox, R. Doering, C. Kampschoer, and C. Herzenberg, "Calibration of Flow and Feedrate Meters In Situ by Means of Pulsed Neutron Activation," Argonne National Laboratory report ANL-80-62, CONF-800602 (1980).

3. P. Kehler, "Two-Phase Flow Measurement by PNA Techniques," Argonne National Laboratory report ANL-NUREG-CT-78-17 (1979).

4. P. Kehler, "Measurement of Slow Flow Velocities by the Pulsed Neutron Activation Technique," Review Group Conference on Advanced Instrumentation Research for Reactor Safety, held at Oak Ridge National Laboratory, July 29-31, 1980, NUREG/CT-0015.

5. A. C. Raptis and S. H. Sheen, "Ultrasonic Properties of Coal Slurries and Flow Measurements by Cross Correlation," IEEE Trans. Sonics and Ultrasonics SU-28, p. 248 (1981).

6. S. H. Sheen and A. C. Raptis, "HYGAS Coal-Slurry Mass-Flow Measurements Using Ultrasonic Cross-Correlation Techniques," Argonne National Laboratory report ANL/FE-49622-TM07 (1979).

7. J. P. Bobis, W. E. Brewer, J. R. McQuinn, N. M. O'Fallon, and R. J. Armani, "Performance Characteristics of a Capacitive Flowmeter on the ANL Solid/Gas Flow Test Facility," Argonne National Laboratory report ANL-82-62, CONF-820612 (1982).

8. H. B. Karplus, A. C. Raptis, and D. R. Canfield, "Development of Testing of High Temperature Acoustic Doppler Flowmeter," Argonne National Laboratory report ANL/FE-81-64 (Sept. 1980).

9. H. B. Karplus and A. C. Raptis, "Flow Measurement of Dense Slurries Using the Sonic Doppler Principle," IEEE Ultrasonics Conf. No. 78, CH 1344-ISU (1978).

10. H. B. Karplus, "Ultrasonic Transducer with Laminated Coupling Wedge," Patent No. 3973152.

11. H. B. Karplus, "High Temperature Transducers for LMFBR Ultrasonic Flowmeters," Argonne National Laboratory Technical Memorandum ANL-CT-77-6.

APPENDIX A. CIRCUIT DETAILS

The basic operating principle of the ANL Doppler Flowmeter is given in Sec. 2 of the report; here details are provided, giving the design philosophy and information needed for a better understanding, and for adjustment and maintenance. An overall view of the main circuit board is given in Fig. A.1; the circuit diagrams of the main board are shown in Figs. A.2-A.4. A single clearly labeled connection between A.2 and A.3 and between A.3 and A.4 shows the interconnection between these circuits. Figure A.4 shows the circuit as it was used at H-coal before modifications. Some modifications subsequently incorporated in units with serial numbers 105 and 111 are shown in Fig. A.5.

The circuit (Fig. A.2) shows a quartz-crystal-controlled oscillator. The plug and socket connected crystal is exchanged readily for operation at a different frequency. Removing the crystal and inserting special coupling circuit (described below) permits operating the unit synchronously with an adjacent unit; the coupling circuit simply plugs into the crystal socket. Controls P1 and P2 feed the oscillator signal to the mixer and power amplifier. The power amplifier VN67AF drives the cable to the sound-transmitting transducer. The same signal controlled by P1 and buffered by Q1 drives the "local oscillator" terminal of the mixer, SRA-3 Terminal 7. The level as adjusted at P1 can be monitored at TP2. About 0.6 V_{p-p} with just noticeable flattening of the sine wave gives SRA3 performance close to optimum. The output of the power amplifier can be monitored at the drain (D) of the FET F1 or at the large 2-W 68-ohm resistor. About 25 V_{p-p} is appropriate at this point.

The received acoustic signal can be monitored at TP 3, where both 5 V.DC as well as the signal is observed. The 5 V.DC powers the remote preamplifier (Fig. A.6) with inductance-capacitance coupling separating the DC power from the AC signal. A step-down transformer T2-1 couples the 95-ohm input line (R62/U) to the 50-ohm input of the SRA-3 mixer. Testpoint TP-1 shows this input.

The mixer yields both sum and difference frequencies of the received signal and the local oscillator. The sum frequency is removed with a three-pole filter and the difference frequency is amplified by op-amp IC1. This amplified signal is passed through a PC board switch to the next section of the circuit (Fig. A.3) at TP 4. The PC board switch permits connecting the rest of the circuit to an external calibration signal instead of the Doppler signal. This external signal is buffered by the unity gain op amp, also part of IC1. (In the original design, instead of a P.C. board switch, leads with colors marked were taken to the front panel DIP switch. DIP Switch 7 was used for calibration and Switch 8 for normal operation. This convenient operation led to a slightly higher noise pickup and was modified in all units except S/N 101 and 103.)

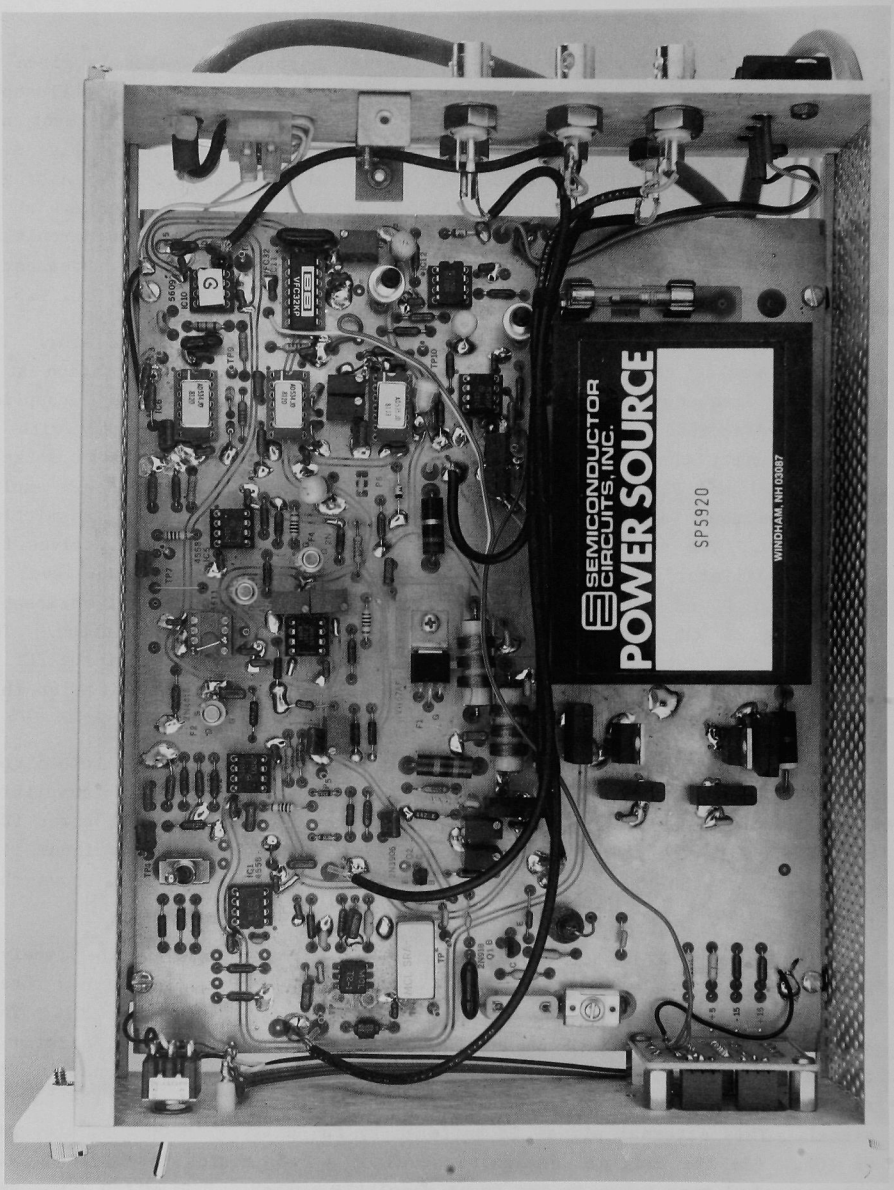

Fig. A.1. Main Circuit Board of ANL Doppler Flowmeter.

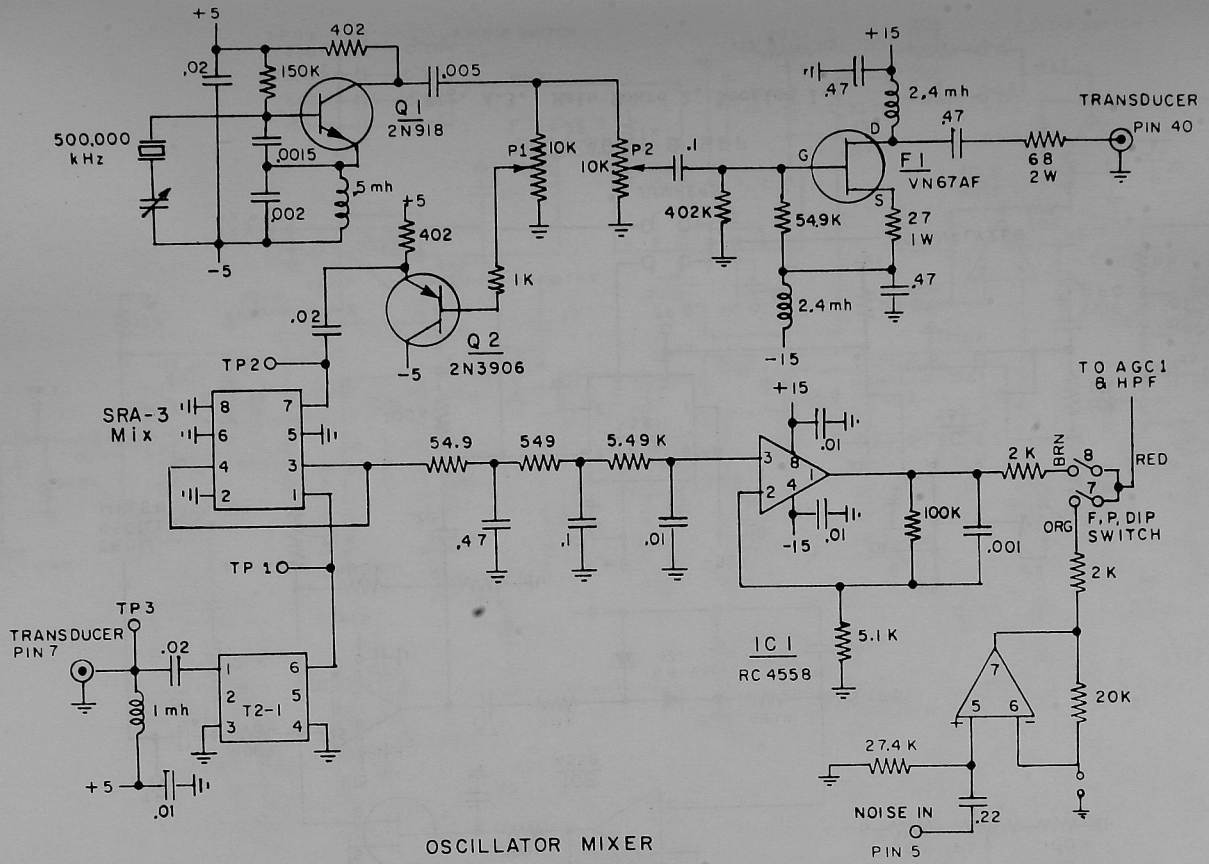

Fig. A.2. Main Board Power Supply.

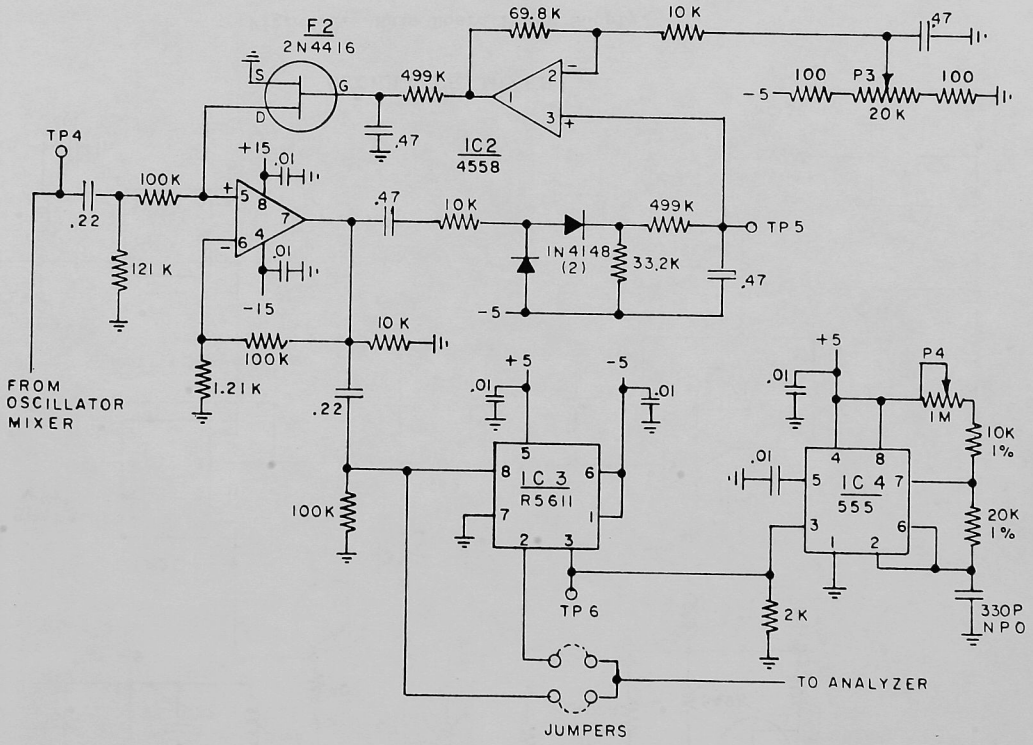

AGC 1 & HPF

Fig. A.3. Main Board 2, Section 1.

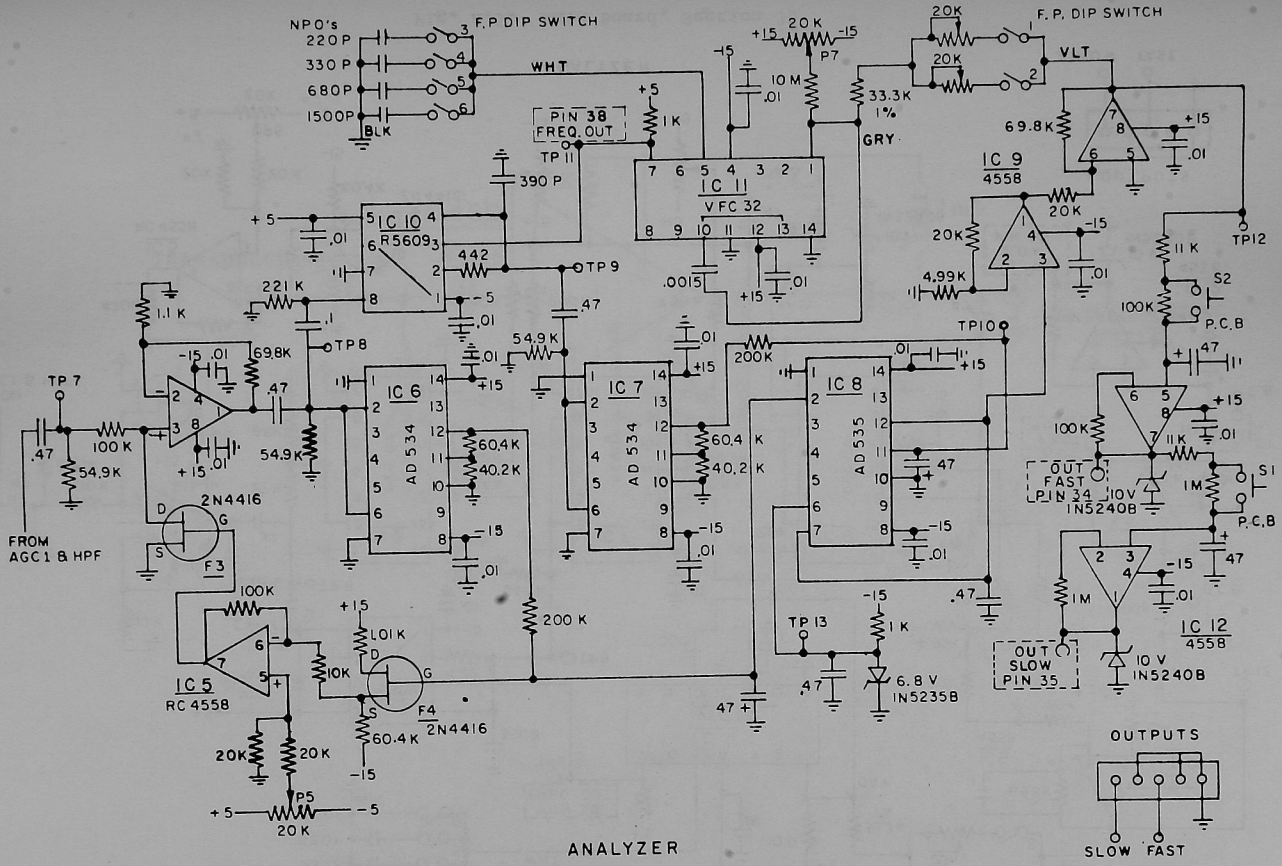

ANALYZER

Fig. A.4. Main Board 3, Section 3a.

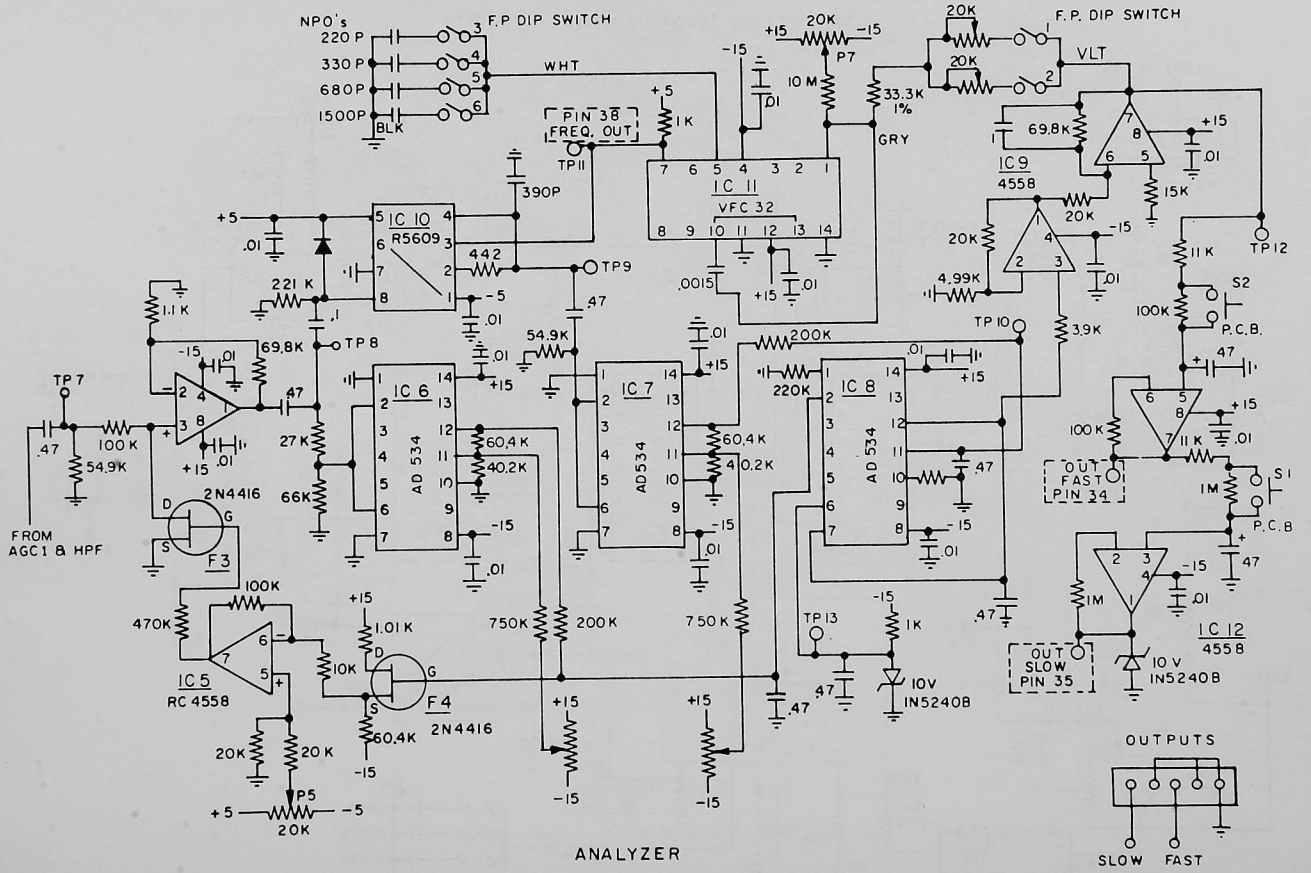

Fig. A.5. Main Board, Section 3b

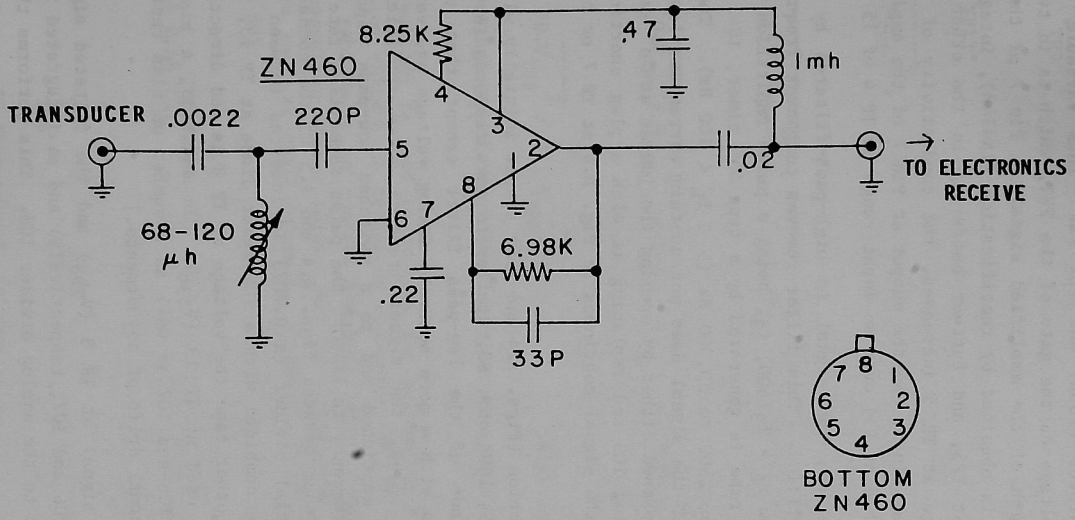

Fig. A.6. Remote Amplifier.

The signal routing beyond TP 4 (Fig. A.3) is to an automatic gain control consisting of a resistor (100k) and FET F2. This variable attenuator is controlled by the voltage on the gate of the FET, which is in turn controlled by the signal strength of the amplified signal at Pin 7 of the op amp IC2. The signal strength is obtained by rectification (IN4148), integration (499K-0.47 μF), as seen at TP5, and further buffering in the other amplifier of IC2. As the voltage at TP 5 increases, the conductivity of F2 increases, reducing the signal at Pin 5. So the output at Pin 7 of the amplifier remains close to 1V (adjustable at P3) over an input range at TP 4 of 15 mV to 3 V.

After amplification, the signal is high-pass-filtered by the switched capacitor filter R5611:IC3. This filter removes component frequencies of the signal that are below $f_L = f_3/500$, f_3, being a pulse repitition rate on Pin 3 of IC3. This pulse rate is generated by a type 555 timer, IC4. The rate is adjustable by P4 from 2500 to 50,000 Hz ($5 < f_L < 100$ Hz). The rate can be monitored at TP6. If the signal does not contain extraneous low frequencies, the filter can be bypassed either by opening the jumper at "a" and closing one at "b", or by removing IC3 and replacing it with a plug shorting Pins 2 and 8. From this point the signal continues to Fig. A.4 at TP 7 or A.5, depending on the unit.

The analyzer section (Figs. A.4 and A.5) starts initially with an automatic gain control, IC5, 100K ohm, F3, similar in many respects to the automatic gain control in front of the low-pass filter except that the two-diode rectifier is replaced with a more accurate analog voltage squarer IC6. Level is adjusted by P5. Also, the signal branches after amplification to the squarer IC6 already mentioned and to a switched low-pass capacitor filter IC10, whose cutoff frequency is $1/100^{th}$ the pulse repetition rate generated by VFC 32. [One difference between Figs. A.4 and A.5 is the connection to IC6. In one case a potential divider (x 0.707) is inserted between TP 8 and the input to IC6; this is combined with a 10V zener diode at TP 13, i.e. pin 6 of IC8, (V_{13a}). In the other case the voltage at TP 8 is fed directly to IC6 and a 6.8 volt zener is used at TP 13 (V_{13b}). In addition, a bias control is shown for Pin 11 of IC6 and IC7 as well as a number of bias resistors at IC8 and IC9 to reduce thermal drift of adjustments.]

Both the input signal at TP 8 (V_{TP8}) and the filtered signal at TP 9 (V_{TP9}) are squared (IC6 and IC7, respectively) and an integrated 200K ohm-47μF capacitor and brought to the analog divider IC8. This performs the operation

$$V_{12} = 10.V_{11}/(V_2 - V_6), \qquad (A.1)$$

where the subscripts refer to the pin numbers on IC8. Now

$$V_{11} = \overline{(V_{TP9})^2}, \qquad (A.2)$$

$$V_6 = V_{TP13}, \qquad (A.3)$$

$$V_2 = \overline{(V_{TP8})^2}, \quad \text{(Fig. A.5)} \qquad (A.4a)$$

and

$$V_2 = \overline{(0.708\ V_{TP8})^2}, \quad \text{(Fig. A.4)} \qquad (A.4b)$$

yielding

$$V_{12} = 10.\overline{V_{TP9}^2} / \overline{V_{TP8}^2} - 6.8 \quad \text{(Fig. A.5)} \qquad (A.5a)$$

and

$$V_{12} = 10.\overline{V_{TP9}^2} / 0.5\ \overline{V_{TP8}^2} - 10. \quad \text{(Fig. A.4)} \qquad (A.5b)$$

The voltage V_{12} is amplified further by a factor -17.5 in IC9 to yield V_{TP12}.

This voltage is used to control the output repetition rate of pulses of the precision voltage to frequency converter VFC 32: IC11 to yield a control repetition rate F_{TP11} to control the high cutoff frequency of the R5609, the switched capacitor filter IC10. Now the large gain in the feedback circuit will assure that at equilibrium V_{12} is small so that substituting $V_{12} = 0$ in Eq. A.5 we get

$$\overline{V_{TP9}^2} \doteq 0.68\ \overline{V_{TP8}^2} \quad \text{(Fig. A.5)} \qquad (A.6a)$$

and

$$\overline{V_{TP9}^2} = 0.5\ \overline{V_{TP8}^2}. \quad \text{(Fig. A.4)} \qquad (A.6b)$$

Further, the cutoff frequency F_c of IC10 is equal to $F_{TP11}/100$.

Thus, $F_{TP11} = 100\ F_d$, where F_d is related to the total Doppler spectrum as a sort of average frequency, being defined as the frequency below which there is exactly 0.68 or 0.5 (Figs. A.5 and A.4) times the total energy in the spectrum. These theoretical numbers are not exactly borne out in practice and

were determined by calibration. The discrepancy is attributed to the high residual input current requirements of the divider IC8 fed by the high-impedance (200K ohm) integrators. As a circuit improvement, the passive integrator should be replaced by active integrators that are less affected by circuit loading.

Besides yielding a frequency output $F_{TP11} = F_o = 100\ F_D$, the circuit also yields a Voltage V_{TP12}, which is very accurately related to F_o. The relation between V_{TP12} and F_{TP11} is precise and linear and adjustable with front panel switches 1-6 and the variable resistor labeled 1, 2, either of which can be selected by closing the correspondingly labeled switch. Switches 3, 4, 5, and 6 select different capacitors. The range of frequencies corresponding to the minimum and maximum selected values of the front panel variable resistors is given as Table 3.

The voltage V_{TP12} is further integrated with a 6-s time constant and brought out via a buffer amplifier IC12b. An additional integrator with a 60-s time constant IC12a is brought out at terminal "slow". This terminal is also protected with a 10-V zener diode to protect external equipment from the 14.5 V maximum. The slow output is to be used by data aquisition systems that sample only once or twice per minute. Data that are not integrated for periods longer than the sampling interval will exhibit aliased fluctuations that are eliminated most easily by the integration scheme described.

Synchronous operation of several units is accomplished by the addition of coaxial cables connecting the rear connector with a miniature circuit board plugging directly into the crystal socket. Units 102 and 103 contain a capacitor potential divider consisting of two 330 F capacitors. Units 104 and 111 have a frequency divider MFC 6020 and tuned LC filter to replace quartz crystal. These circuits are shown in Fig. A.7.

Tube backplane wiring connecting the units together and to the readout meters is shown in Fig. A.8.

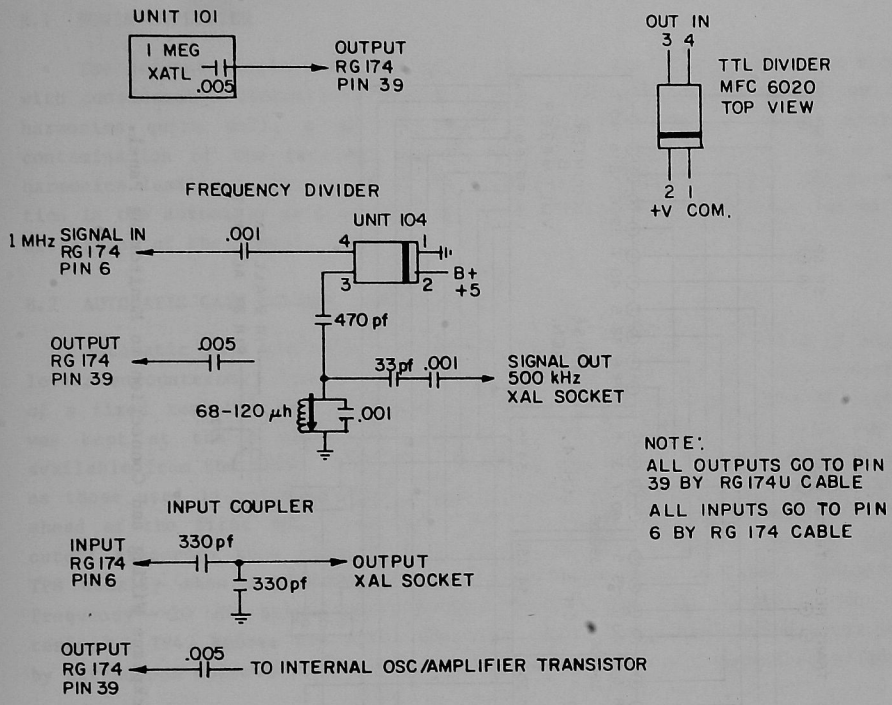

Fig. A.7. Modifications for Multiple Unit Synchronous Operation.

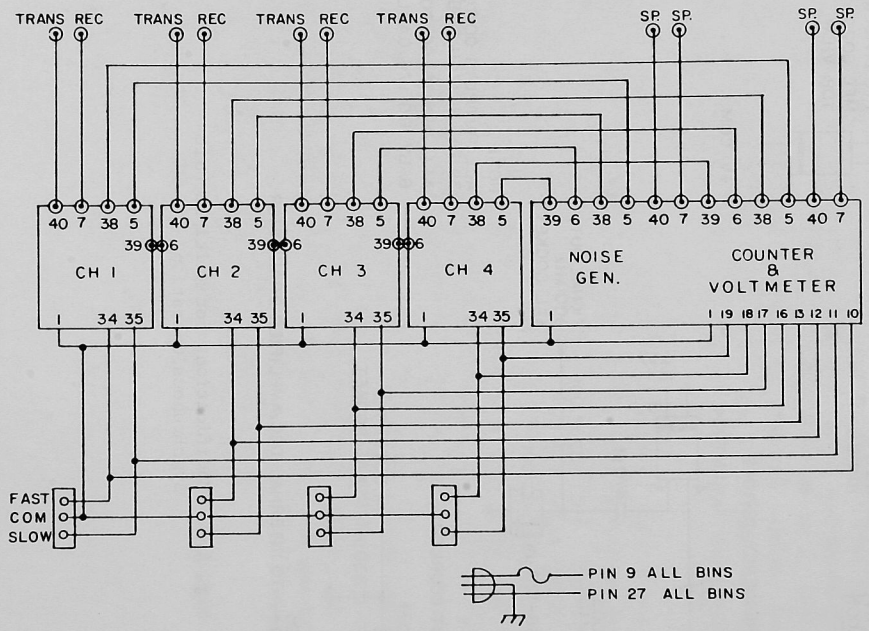

Fig. A.8. Backplane Wiring and Connection to Monitoring Panel.

APPENDIX B. RECOMMENDED DESIGN CHANGES

After constructing and calibrating several units, we have observed that several aspects of the ultrasonic Doppler flowmeter could be improved.

B.1 POWER AMPLIFIER

The present single-ended design of the power amplifier leads to a signal with considerable distortion. Although the tuned transducers filter out the harmonics quite well, a more sinusoidal excitation would reduce possible contamination of the received signal with some Doppler signals due to the harmonics leading to harmonics of the Doppler. At this time harmonic generation in the automatic gain control (ca 1% - 20dB) exceeds the level due to the distortion of the signal.

B.2 AUTOMATIC GAIN CONTROL (AGC)

Automatic gain controls were needed because of the wide range of signal levels encountered. Some distortion is introduced by the circuit consisting of a fixed resistor and FET working as a potential divider. The distortion was kept at the 1% level by selecting FETs. Superior circuits may be available from the audio industry. Probably there are circuits available such as those used in portable tape recorders. Spectra taken at test Point TP 4, ahead of the first AGC, show less relative noise in the region beyond the cutoff frequency than spectra taken after the AGC. Spectra taken at TP7 or TP8 usually show a plateau from the cutoff frequency to about twice that frequency——~20 dB below the spectrum level below the cutoff level. At testpoint TP4, before the first AGC, the level beyond the cutoff is governed by extraneous noise in the system and usually extends well beyond 30 or 40 dB.

B.3 ANALYZER SECTION

In the analyzer section, individual offset controls were added to the divider, permitting balancing the output for low input levels and allowing the units to operate with reduced signal level. But this improvement was limited (~2 dB). Two improvements seem to be called for:

One improvement eliminates the high output impedance of the integrator by substituting an active integrator for the passive integrator; this may well include a two-pole or even a three-pole low pass filter, and

The other is the replacement of the squaring circuit AD 534 by a RMS to DC converter such as the AD 536A; the RMS voltage falls much more slowly with reduced signal levels than the square.

The system will work quite well even with a simple rectifier circuit instead of the true squarer or RMS system used here. Ultimately, when component cost becomes important, an active rectifier would be somewhat cheaper than the squarer, and since the divider simply compares two very similar signals, the error might well be negligible. Further considerations of minor economics of this nature are beyond the scope of this report.

B.4 SIGNAL LOSS ALARM

Low signal levels lead to amplification of system noise, leading to full-scale output. Some form of alarm is needed to eliminate this false indication.

Distribution for ANL/FE-85-14

Internal:

W. E. Brewer
J. P. Bobis
T. N. Claytor
E. D. Doss
W. A. Ellingson
P. S. Farber
N. Gopalsami
R. E. Holtz
H. B. Karplus
A. B. Krisciunas
W. P. Lawrence
L. G. LeSage
T. P. Mulcahey
K. M. Myles
N. M. O'Fallon
M. Petrick
W. F. Podolski
K. G. Porges
A. C. Raptis (10)
S. H. Sheen
C. E. Till
R. S. Zeno
S. K. Zussman
ANL Contract File
ANL Libraries
ANL Patent Dept.
TIS Files (5)

External:

DOE-TIC, for distribution per UC-90a (160)
Manager, Chicago Operations Office, DOE
F. Herbaty, DOE-CH
M. Zahid, DOE-CH
Components Technology Division Review Committee:
P. Alexander, Flopetrol Johnston Schlumberger, Houston
D. J. Anthony, General Electric Company, San Jose
A. A. Bishop, U. Pittsburgh
B. A. Boley, Northwestern U.
R. N. Christensen, Ohio State U.
R. Cohen, Purdue U.
R. E. Scholl, URS, San Francisco
J. Weisman, U. Cincinnati
D. L. Basdekas, Office of Nuclear Regulatory Research, USNRC
J. Carr, Office of Fossil Energy, USDOE
C. S. Chen, U. Akron
J. S. Coleman, Office of Energy Research, USDOE
S. Dapkunas, Office of Fossil Energy, USDOE
A. C. Dolbec, Electric Power Research Institute, Palo Alto
P. J. Ebert, Office of Energy Research, USDOE
M. Hobday, Morgantown Energy Technology Center, USDOE
J. Hickerson, Pittsburgh Energy Technology Center, USDOE
F. Karlson, Electric Power Research Institute, Palo Alto
T. Keech, Morgantown Energy Technology Center, USDOE
J. Kovach, Morgantown Energy Technology Center, USDOE
S. Lee, Pittsburgh Energy Technology Center, USDOE
A. Liberatore, Morgantown Energy Technology Center, USDOE
J. Notestein, Morgantown Energy Technology Center, USDOE
W. H. Piispanen, Battelle-Columbus Laboratories
S. Sami, Southern Illinois U., Carbondale
T. Schmidt, Shell Development, Houston
J. F. Schooley, National Bureau of Standards, Washington, D.C.
M. A. Scott, U. Tennessee Space Institute, Tullahoma
F. E. Senftle, U.S. Geological Survey, Washington, D.C.
T. Simpson, Office of Fossil Energy, USDOE
L. D. Strickland, Morgantown Energy Technology Center, USDOE
A. B. Tanner, U. S. Geological Survey, Washington, D.C.
O. Tassicker, Electric Power Research Institute, Palo Alto
E. S. Van Valkenburg, Leeds & Northrup Co., North Wales, PA
J. Wilson, Morgantown Energy Technology Center, USDOE